NUCLEAR RECEPTOR CONTROLS NEMATODE METABOLISM AND DEVELOPMENT: INSIGHT INTO MAN'S NEMESIS, THE CONQUEROR WORM

APPROVED BY SUPERVISORY COMMITTEE

David J. Mangelsdorf, Ph.D.

Richard J. Auchus, M.D., Ph.D.

Leon Avery, Ph.D., M.B.A.

David W. Russell, Ph.D.

Steven A. Kliewer, Ph. D.

DEDICATION

I would like to thank the members of my graduate committee

For my parents and wife

For their endless support and encouragement

ACKNOWLEDGEMENTS

I am grateful to numerous people that have supported and helped me for the complete my Ph. D. studying. I owe my deepest gratitude to my thesis advisor, Dr. David Mangelsdorf, who gave me the opportunity to work under his supervision. David is absolutely one of the top scientists I have ever met. He has terrific taste in science and always concentrates on the most significant questions, which, in my case, gave me exhilarating research projects to work on. David has the magic to make people enjoy working with him, which allowed me to find lots of collaborators to go through the difficulties I had with my experiments. I also truly appreciate his patience and the independence he gave to me. In the past four years, David has instilled in me the merits of a successful scientist, which I believe critical for my future success.

It was very fortunate to work with Dr. Young-jai You, who was a post-doc of Dr. Leon Avery's lab, and is now an assistant professor at Virginia Commonwealth University. Her expertise and knowledge in *C. elegans* research helped me a lot. This was particularly important for a person like me as I had no experience *C. elegans* when I started.

Collaborators at UTSW and elsewhere have substantially contributed to my research. Dr. Daniel Motola, a previous student, pioneered the DAF-12 research in our lab and left this intriguing project to me. Dr. Richard Auchus and his post-doc Dr. Kamalesh Sharma at UTSW has worked tirelessly to made chemicals for

me. Dr. Eric Xu at Van Andel Institute and his lab members Drs. Eric Zhou, Kelly Suino-Powell, Aoife Conneely, and Craig Ogata, finished the crystallographic study of the parasite DAF-12. Drs. John Hawdon and Xin Gao at George Washington University and Dr. James Lok at University of Pennsylvania helped me with the parasite experiments. Dr. Greg Tylka at Iowa State University collected *H. glycines* samples, from which Ms. Daphne Head in Dr. David Russell's lab (UTSW) helped me to make the cDNA library. The *C. elegans* Genome Center at University of Minnesota and Dr. Adam Antebi at Baylor College of Medicine provided me the *C. elegans* trains. The high-throughput screening core of UTSW has helped in the initial screening of DAF-12 ligands. I also want to thank for the hard work put forth by the rotation students Nam Nguyen, David Reading and Nathaniel Schaffer, and Angie Bookout and Nathaniel Schaffer for reading the dissertation draft. This dissertation would not have been possible without their involvement.

I would like to send my sincere gratitude to my dissertation committee, which is composed of Dr. Richard Auchus (chair), Dr. Leon Avery and Dr. David Russell, as well as Dr. Steven Kliewer, the co-PI of our laboratory. They has made their support available in a number of ways, including giving me thoughtful advice, and enthusiastically offering help with my experiments.

I want to thank my colleagues in the Mango/Kliewer lab for all their support, spirit, and friendship. It was a pleasure to come to lab everyday and work

with these people. I also want to thank Gail Wright, Aurora Del Rosario and Ewa Borowicz for their administrative help.

Finally, I am heartily thankful to my family. My parents, Feng, my father, and Lanying, my mother, gave me the best education and upbringing they could from the very beginning of my life. They always stay with me, support and encourage me whenever I am suffering from difficulties. Especially, I want to thank my wife, Min, for her love, support, and sweetness. I feel so fortunate to have them in my life.

NUCLEAR RECEPTOR CONTROLS NEMATODE METABOLISM AND DEVELOPMENT: INSIGHT INTO MAN'S NEMESIS, THE CONQUEROR WORM

by

ZHU WANG

DISSERTATION

Presented to the Faculty of the Graduate School of Biomedical Sciences

The University of Texas Southwestern Medical Center at Dallas

In Partial Fulfillment of the Requirements

For the Degree of

DOCTOR OF PHILOSOPHY

The University of Texas Southwestern Medical Center at Dallas

Dallas, Texas

November, 2010

NUCLEAR RECEPTOR CONTROLS NEMATODE METABOLISM AND DEVELOPMENT: INSIGHT INTO MAN'S NEMESIS, THE CONQUEROR WORM

ZHU WANG, Ph.D.

The University of Texas Southwestern Medical Center at Dallas, 2010

Supervising mentor: David J. Mangelsdorf, Ph.D.

The nuclear receptor DAF-12 plays a central role in controlling the larval development of *C. elegans*. Activation of DAF-12 by its ligands called dafachronic acids (DAs) commits the nematode to development into reproductive adult, which will otherwise arrest at a diapause stage called dauer. But the molecular mechanisms remain unclear. Furthermore, whether the DAF-12 signaling pathway is conserved in other nematode species, especially parasitic ones, is also unknown.

One aspect of my studies is to investigate the molecular mechanisms by which this DA-DAF-12 signaling pathway regulates the *C. elegans* development. By measuring a series of metabolic parameters, we demonstrated that DAF-12 activation markedly elevated aerobic utilization of fatty acids. In accordance with this, expression of a network of metabolic genes responsible for energetic catabolism of fatty acids was up-regulated as well. Importantly, inhibition of these metabolic genes abolished the reproductive growth stimulated by DAF-12. These results revealed a DAF-12-controlled metabolic network that coordinates energy metabolism and larval development in *C. elegans*.

The other emphasis of my work is on the role of DAF-12 in parasitic nematodes. Our results showed that, as seen in *C. elegans*, DAF-12 activation also induced recovery from the infective L3 (iL3), which is the dauer larva of the parasites. Moreover, the metabolic genes controlled by *C. elegans* DAF-12 were identified in parasitic nematodes. These facts indicate that the DAF-12 signaling pathway is conserved in parasitic nematodes. Importantly, administration of DA dramatically reduced the formation of the pathogenic larvae that are mostly resistant to current anthelmintic drugs, indicating the unique therapeutic potential of DAF-12 ligands to treat nematode parasitic diseases. To understand the pharmacology of targeting DAF-12, we solved the 3-demenstional structure of DAF-12 in a parasitic nematode called *Stronglyloides stercoralis* that infects human. These results reveal the molecular basis for DAF-12 ligand binding and identify DAF-12 and its downstream metabolic genes as unique therapeutic targets in parasitic nematodes. Based on this, we have discovered several small molecules that activate

Stronglyloides stercoralis DAF-12 and these molecules may provide lead compounds for developing novel anthelmintic drugs.

TABLE OF CONTENTS

PRIOR PUBLICATIONS

Wang, Z., You, Y., Kliewer, S.A., Mangelsdorf, D.J. Conserved Nuclear Receptor Signaling Pathways Mediate Nutrient Responses that Coordinate Energy Metabolism and Larval Development of *C. elegans*. (Manuscript in preparation).

Wang, Z., Zhou, X.E., Motola, D.L., Gao, X., Suino-Powell, K., Conneely, A., Ogata, C., Sharma, K.K., Auchus, R.J., Lok, J.B., Hawdon, J.M., Kliewer, S.A., Xu, H.E., Mangelsdorf D.J. Identification of the Nuclear Receptor DAF-12 as a Therapeutic Target in Parasitic Nematodes. *Proc Natl Acad Sci U S A.* 2009 Jun 9; 106(23):9138-43.

Sharma, K.K.*, **Wang, Z.***, Motola, D.L., Cummins, C.L., Mangelsdorf, D.J., Auchus, R.J. Synthesis and Activity of Dafachronic Acid Ligands for the *C. elegans* DAF-12 Nuclear Hormone Receptor. *Mol Endocrinol.* 2009 May:23(5):640-8.

Bethke, A., Fielenbach, N., **Wang, Z.**, Mangelsdorf, D.J., Antebi, A. Nuclear Hormone Receptor Regulation of microRNAs Controls Developmental Progression. *Science.* 2009 Apr 3;324(5923):95-8.

Lefterov, I., Bookout, A., **Wang, Z.**, Staufenbiel, M., Mangelsdorf, D.J., Koldamova, R. Expression Profiling in APP23 Mouse Brain: Inhibition of Aβ Amyloidosis and Inflammation in Response to LXR Agonist Treatment. *Mol Neurodegener.* 2007 Oct 22;2:20.

Wang, Z., Cummins, C.L., Motola, D.L., Mangelsdorf, D.J. Bile Acid-like Hormones Function as Ligands for the Nematode Orphan Nuclear Receptor DAF-12 and Govern Dauer Formation, reproduction and lifespan. In: *Bile Acids: Biological Actions and Clinical Relevance—Falk Symposium 155*, 2007 (Review).

*, co-first author

LIST OF FIGURES

LIST OF TABLES

LIST OF ABBRIAVATIONS

DA, dafachronic acid

daf, abnormal dauer formation

daf-c, constitutive dauer formation

daf-d, dauer defective

qPCR, quantitative Real-time polymerase chain reaction

EMSA, electrophoretic mobility shift assay

C. elegans, Caenorhabditis elegans

A. caninum, Ancylostoma caninum

A. ceylanicum, Ancylostoma ceylanicum

N. americanus, Necator americanus

S. stercoralis, Strongyloides stercoralis

H. glycines, Heterodera glycines

H. contortus, Haemonchus contortus

ASP, *Ancylostoma*-secreted protein

CHAPTER ONE

Conserved Nuclear Receptor Signaling Pathways Mediate a Nutrient Responses that Coordinate Energy Metabolism and Larval Development in *C. elegans*

1.1 INTRODUCTION

Nematodes conduct their larval development in accordance with their living environment. In favorable conditions with abundant nutrients, the free-living nematode *C. elegans* undergoes reproductive growth continuously from embryo to fertile adult through four larval stages (L1-L4). In contrast, as the population grows and the nutrient supply becomes limited, the worm halts the reproductive growth and enters an alternative L3-diapause stage termed the dauer, which is characterized by its unique features of autonomy, stress-resistance, and extended lifespan. These characteristics ensure the animal can survive the environmental challenges. Ambient temperature is the other environmental cue that *C. elegans* evaluates to make the development decision, with the tendency to form dauer at higher temperature, when lifecycle is executed more quickly and thus better nutrient supply must be available (Riddle and Albert, 1997).

The nuclear receptor DAF-12 plays a central role in controlling this nutrient-controlled nematode development. In *C. elegans*, it is activated by its cognate ligands named dafachronic acids (DAs). These steroid hormones are physiologically made by the cytochrome P450 (CYP450) DAF-9 as an output of the environmentally-regulated insulin/IGF-I (II-S) and TGF-β signaling pathways. By inducing transcription of various genes, DAF-12 activation leads to commitment of the worm development to reproduction (Motola et al., 2006; Sharma et al., 2009). Under harsh environments, however, DAs are

absent and the ligand-free DAF-12 recruits transcriptional co-repressors such as DIN-1, which instead drives dauer formation (Ludewig et al., 2004b).

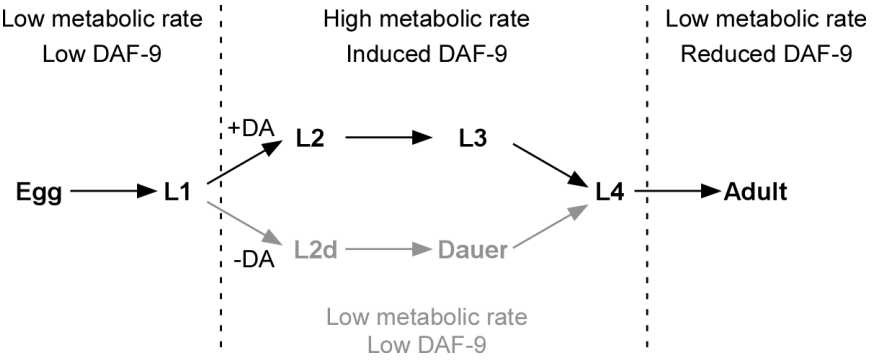

Figure 1-1. Correlation of Energy Metabolism and DAF-12 Activity during *C. elegans* Larval Development

During different developmental stages, *C. elegans* exhibits distinct energy metabolism. Embryos and L1 larvae have relatively low rates of energy metabolism and preferentially use the anaerobic glyoxylate pathway to consume their lipid storage. Once committed to reproductive growth, the worms shift their metabolism to a highly aerobic mode in which TCA-cycle activity is substantially increased until growth is complete and adulthood is reached. This shift enables the larvae to actively utilize ingested nutrients and support the rapid, energy-consuming reproductive growth. This metabolic shift, however, does not occur when the worms are diverted to dauer diapause (Braeckman et al., 2009; Riddle and Albert, 1997). Interestingly, the changes in energy metabolism during larval development are accompanied by an alteration of the expression of DAF-9, the enzyme that make DAs (Gerisch et al., 2001). These facts clearly show a correlation between DAF-12 activity and energy metabolism during *C. elegans* larval development (Figure 1-1).

From the perspective of evolutionary biology, it is very likely that the DAF-12 signaling pathway regulates energy metabolism in response to environmental nutrients (Figure 1-2A). In the fed state when the insulin signaling pathway is active, the mammalian homologs of DAF-12 liver X receptors (LXRs) (Mooijaart et al., 2005), are activated by oxysterols. Like DAF-12 ligands, these physiological ligands of LXRs are made from cholesterol by a group of CYP450s. As a result, LXR activation causes enhanced hepatic lipid deposition and improved utilization of dietary lipids by peripheral tissues (Kalaany and Mangelsdorf, 2006). In the fruit fly, DAF-12 has a homolog called *Drosophila* nuclear hormone receptor 96, or DHR96. Loss of this nuclear receptor confers on flies susceptibility to starvation and resistance to diet-induced obesity, resulting from dysregulation of a gastric triglyceride lipase (Sieber and Thummel, 2009). Thus far, DHR96 ligands and the CYP450s responsible for their production remain unknown. However, the fact that this nuclear receptor is able to bind cholesterol *in vitro* (Horner et al., 2009) strongly suggests its physiological ligands are cholesterol metabolites.

Previously, DAF-12 was reported to promote L3 stage-specific seam-cell patterning by regulating heterochronic genes, which uncovered DAF-12's function in cell fate determination (Bethke et al., 2009; Hammell et al., 2009). In this study, we focused on DAF-12's metabolic function. We found that lipid storage was suppressed while oxygen consumption was stimulated by DA administration. Meanwhile, *C. elegans* reproductive growth was also accelerated, indicating that DAF-12 can promote aerobic catabolism of lipids to support reproductive growth. Further studies proved that DAF-12 could regulate various genes involved in lipid metabolism, either by directly binding gene

promoters or by indirect mechanisms. Finally, using a specific inhibitor and RNAi technology, we demonstrated that the lipid utilization is required for DAF-12 to promote *C. elegans* reproductive growth. Our results therefore reveal a gene network for lipid catabolism under the control of DAF-12, which serves as the energetic basis for reproductive growth in *C. elegans*.

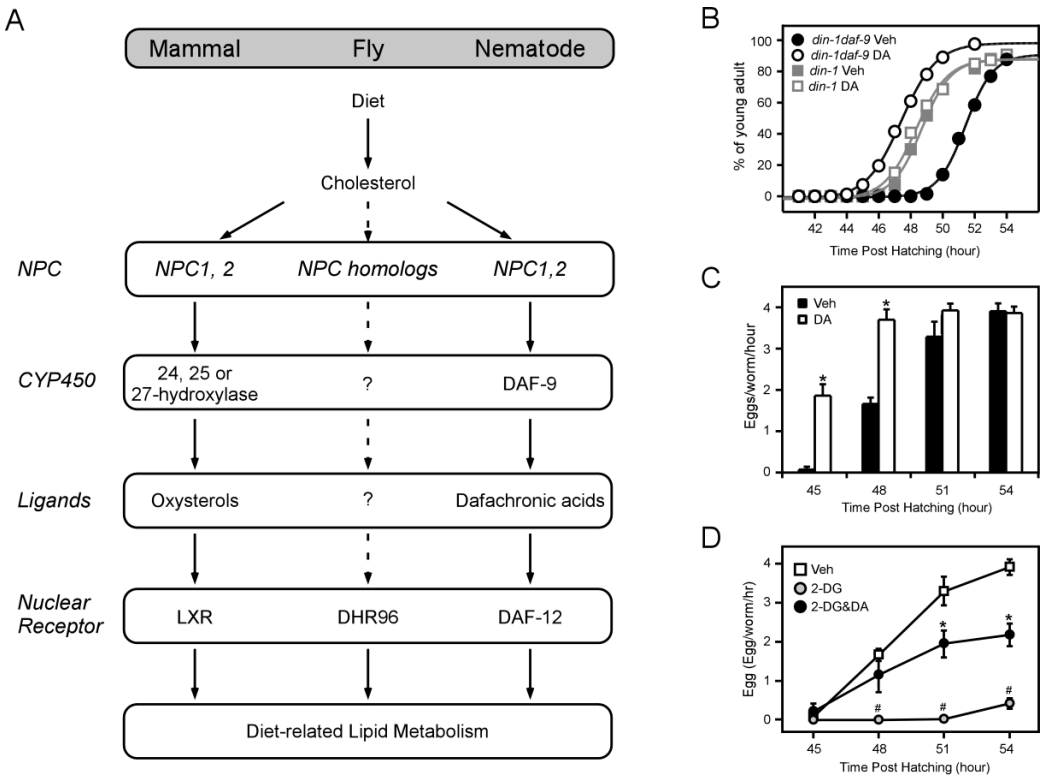

Figure 1-2. DAF-12 Accelerates Reproductive Growth in *C. elegans*

(A) Schematic illustration of conserved nuclear receptor signaling that mediates nutrient response in animals. (B-C) Reproductive growth as measured by developmental transition from L4 larvae to young adults (B), or by egg-laying assay (C). Data are presented as the number of eggs laid by each worm per hour. n=4±s.d. (D) DA rescues the growth delay caused by glucose restriction in *C. elegans*. Reproductive growth was measured as in (C). Veh, ethanol; DA, 200 nM Δ^7-DA; *, p<0.01 by Student t-test, all compared to the vehicle treated worms. #, p<0.01, compared to the 2-DG treated worms. NPC, Niemann Pick type C, the cholesterol transporter.

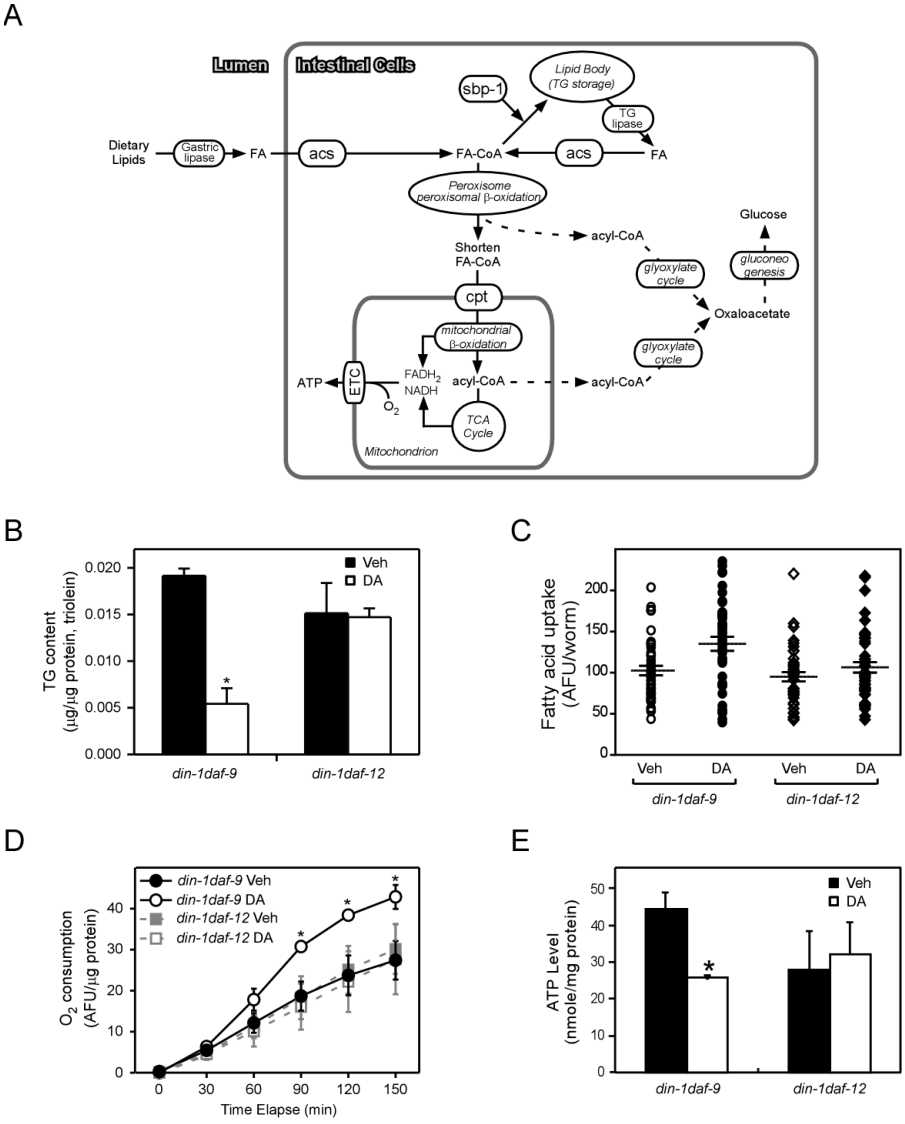

Figure 1-3. DAF-12 Stimulates Aerobic Catabolism of Fatty acids in *C. elegans*

(A) Schematic illustration of lipid metabolism in *C. elegans*. Dashed lines indicate pathways to anaerobic lipid catabolism. (B-E) Triglyceride content (B), dietary fatty acid uptake (C), oxygen consumption (D), and ATP level at steady state (E) were measured in *din-1daf-9* and *din-1daf-12* mutant worms. *, p<0.01 by Student t-test. Data represent at least two (C, E) or four (B, D) independent experiments.

1.2 RESULTS

1.2.1 DAF-12 Enhances Reproductive Growth and Lipid Catabolism in *C. elegans*

DAF-12 activation prevents dauer formation and induces reproductive growth to adulthood in *C. elegans*. However, it is not clear whether the nuclear receptor just makes the developmental decision, or also affects the progress of reproductive growth. To investigate this, we employed *din-1daf-9* mutants, which lack DAF-9 (and hence endogenous DAs) and the DAF-12 transcriptional co-repressor DIN-1 and therefore undergo constitutively reproductive development (Ludewig et al., 2004b). The double mutants provided us with a convenient tool to test the function of DAF-12 specifically during the reproductive growth simply by supplementation of exogenous DAF-12 ligands. We found that reproductive growth of *C. elegans* was accelerated by DAF-12 activation as evidenced by the fact that *din-1daf-9* larvae supplemented with Δ^7-DA developed into young adults (Figure 1-2B), or started laying eggs (i.e. became reproductively mature) (Figure 1-2C) faster than the vehicle treated larvae. Moreover, the *din-1* mutants, which are able to make DA on their own, also grew faster than *din-1daf-9* mutants, indicating that not only pharmacological but also physiological DAF-12 activation could accelerate reproductive growth in *C. elegans*. Interestingly, DA treatment could, to some extent, rescue the reproductive growth delay caused by glucose restriction (Figure 1-2D), suggesting that the acceleration of worm growth stimulated by DAF-12 was probably not a result of regulating carbohydrate metabolism.

We therefore tested whether DAF-12 regulates metabolism of lipids, which are the other major energy source for *C. elegans*. To characterize the role of DAF-12 in lipid metabolism, we first examined the amount of triglyceride (TG), which is the main storage

depot for lipids. We found that Δ^7-DA treatment could decrease the TG content in *din-1daf-9*, but not in *din-1daf-12* mutants that lack DAF-12 expression. This finding revealed that DAF-12 activation could reduce energy storage in *C. elegans* (Figure 1-3B). Since *C. elegans* TGs are dominantly derived from dietary fatty acids (Figure 1-3A), we then assayed fatty acid uptake by these worms. As shown in Figure 1-3C, we were unable to detect a significant effect of DAF-12 on dietary fatty acid uptake, indicating that the decreased TG storage was not due to reduced nutrient intake. This result suggested that fatty acid catabolism could be enhanced. Next, we asked whether an aerobic or anaerobic catabolism of fatty acid was involved, by monitoring oxygen consumption by the worms. We observed elevated oxygen consumption in *din-1daf-9* worms following Δ^7-DA treatment (Figure 1-3D), indicating that DAF-12 could stimulate aerobic catabolism of fatty acids. Interestingly, the steady state concentration of ATP, the immediate form of energy storage, was lower in the DA-treated worms that grew faster (Figure 1-3E, *din-1daf-9*, DA vs Veh), which reveals an enhanced energy requirement for the accelerated reproductive growth (Figure 1-2B and C). Taken together, these results showed that DAF-12 activation could not only commit the worm to the reproductive route of development, as reported previously, but also provide energy for the reproductive growth by stimulating aerobic catabolism of fatty acids.

Table 1-1. Expression of Metabolic Genes in Response to DAF-12 activation

Fatty acid metabolism

Gene ID	Gene Family	Gene Ontology	DA/Veh[a]	Method
sbp-1	SREBP-1c	lipogenesis	0.51	qPCR
HSL-1	Triglyceride lipase	lipolysis	NC	qPCR
K04A8.5	Triglyceride lipase	lipolysis	NC	affy
K08B12.1	Triglyceride lipase	lipolysis	13.75	qPCR
fil-1	Triglyceride lipase	lipolysis	0.37	qPCR
lips-1	Triglyceride lipase	lipolysis	NC	affy
lips-2	Triglyceride lipase	lipolysis	NC	affy
lips-4/fil-2	Triglyceride lipase	lipolysis	NC	affy
lips-6	Triglyceride lipase	lipolysis	4.68	qPCR
lips-7	Triglyceride lipase	lipolysis	NC	qPCR
lips-8	Triglyceride lipase	lipolysis	NC	affy
lips-9	Triglyceride lipase	lipolysis	3.47	qPCR
lips-10	Triglyceride lipase	lipolysis	NC	affy
lips-11	Triglyceride lipase	lipolysis	NC	affy
lips-12	Triglyceride lipase	lipolysis	NC	affy
lips-13	Triglyceride lipase	lipolysis	NC	affy
lips-14	Triglyceride lipase	lipolysis	NC	affy
lips-15	Triglyceride lipase	lipolysis	NC	affy
lips-16	Triglyceride lipase	lipolysis	NC	affy
lips-17	Triglyceride lipase	lipolysis	0.09	qPCR
NHR-49	HNF-4 homolog	lipolysis	NC	qPCR
FASN-1	fatty acid synthase	Fatty acid biosynthesis	2.92	qPCR
F32H2.6	fatty acid synthase	Fatty acid biosynthesis	2.46	qPCR
pod-2	acyl-CoA carboxylase	Fatty acid biosynthesis	NC	qPCR
fat-1	fatty acid desaturease	unsaturated fatty acid	NC	qPCR
fat-2	fatty acid desaturease	unsaturated fatty acid	NC	qPCR
fat-3	fatty acid desaturease	unsaturated fatty acid	NC	qPCR
fat-4	fatty acid desaturease	unsaturated fatty acid	NC	qPCR
fat-5	SCD	unsaturated fatty acid	0.72	qPCR
fat-6	SCD	unsaturated fatty acid	NC	qPCR
fat-7	SCD	unsaturated fatty acid	12.85	qPCR
Y54E5A.1	fatty acid desaturease	unsaturated fatty acid	NC	qPCR
elo-1	fatty acid elongase	fatty acid elongation	NC	qPCR
elo-2	fatty acid elongase	fatty acid elongation	NC	qPCR
elo-4	fatty acid elongase	fatty acid elongation	4.93	qPCR
acs-1	acyl-CoA synthase/ligase	Fatty acid activation	2.02	qPCR

acs-2	acyl-CoA synthase/ligase	Fatty acid activation	0.38	qPCR
acs-3	acyl-CoA synthase/ligase	Fatty acid activation	3.01	qPCR
acs-4	acyl-CoA synthase/ligase	Fatty acid activation	0.63	qPCR
acs-5	acyl-CoA synthase/ligase	Fatty acid activation	NC	qPCR
acs-11	acyl-CoA synthase/ligase	Fatty acid activation	NC	affy
acs-12	acyl-CoA synthase/ligase	Fatty acid activation	NC	affy
acs-13	acyl-CoA synthase/ligase	Fatty acid activation	NC	affy
acs-14	acyl-CoA synthase/ligase	Fatty acid activation	NC	affy
acs-15	acyl-CoA synthase/ligase	Fatty acid activation	NC	affy
acs-16	acyl-CoA synthase/ligase	Fatty acid activation	NC	affy
acs-17	acyl-CoA synthase/ligase	Fatty acid activation	NC	affy
acs-18	acyl-CoA synthase/ligase	Fatty acid activation	0.13	affy
acs-19	acyl-CoA synthase/ligase	Fatty acid activation	NC	qPCR
acs-20	acyl-CoA synthase/ligase	Fatty acid activation	2.23	qPCR
R09E10.4	acyl-CoA synthase/ligase	Fatty acid activation	NC	affy
Y49E10.20	CD36	Fatty acid uptake	NC	affy
acbp-3	acyl-CoA binding protein	Fatty acid binding & transport	2.52	qPCR
lbp-1	fatty acid binding protein	Fatty acid binding & transport	NC	qPCR
lbp-4	fatty acid binding protein	Fatty acid binding & transport	NC	qPCR
lbp-5	fatty acid binding protein	Fatty acid binding & transport	0.45	qPCR
lbp-7	fatty acid binding protein	Fatty acid binding & transport	0.48	qPCR
lbp-8	fatty acid binding protein	Fatty acid binding & transport	0.31	qPCR
F08A8.2	acyl-CoA oxidase, perioximal	fatty acid β-oxidation	6.83	qPCR
F08A8.1	acyl-CoA oxidase, perioximal	fatty acid β-oxidation	NC	qPCR
F08A8.3	acyl-CoA oxidase, perioximal	fatty acid β-oxidation	NC	affy
F08A8.4	acyl-CoA oxidase, perioximal	fatty acid β-oxidation	NC	qPCR
F25C8.1	acyl-CoA oxidase, perioximal	fatty acid β-oxidation	NC	affy
F58F9.7	acyl-CoA oxidase, perioximal	fatty acid β-oxidation	NC	affy
F59F4.1	acyl-CoA oxidase, perioximal	fatty acid β-oxidation	0.65	qPCR
C48B4.1	acyl-CoA oxidase, perioximal	fatty acid β-oxidation	0.46	qPCR
ech-3	enoyl-CoA hydratase, perioximal	fatty acid β-oxidation	NC	affy
ech-8	enoyl-CoA hydratase, perioximal	fatty acid β-oxidation	NC	affy
ech-9	enoyl-CoA hydratase, perioximal	fatty acid β-oxidation	0.54	qPCR
F53A2.7	Long chain fatty-CoA thiolase, perioximal	fatty acid β-oxidation	NC	affy
T05E7.1	Long chain fatty-CoA thiolase, perioximal	fatty acid β-oxidation	2.16	qPCR
cpt-1	CPT-I	fatty acid β-oxidation	0.78	qPCR
cpt-2	CPT-I	fatty acid β-oxidation	NC	qPCR
cpt-3	CPT-I	fatty acid β-oxidation	0.43	qPCR
cpt-4	CPT-I	fatty acid β-oxidation	NC	qPCR

cpt-5	CPT-I	fatty acid β-oxidation	2.49	qPCR
cpt-6	CPT-I	fatty acid β-oxidation	4.39	qPCR
acdh-2	acyl-CoA dehydrogenase	fatty acid β-oxidation	0.26	qPCR
acdh-3	acyl-CoA dehydrogenase	fatty acid β-oxidation	NC	affy
acdh-7	acyl-CoA dehydrogenase	fatty acid β-oxidation	NC	affy
acdh-8	acyl-CoA dehydrogenase	fatty acid β-oxidation	NC	affy
acdh-10	acyl-CoA dehydrogenase	fatty acid β-oxidation	NC	qPCR
K09H11.1	acyl-CoA dehydrogenase	fatty acid β-oxidation	NC	affy
ech-1	enoyl-CoA hydratase / 3-hydroxyacyl-CoA dehydrogenase	fatty acid β-oxidation	NC	qPCR
ech-2	enoyl-CoA hydratase	fatty acid β-oxidation	NC	affy
ech-4	enoyl-CoA hydratase /isomerase	fatty acid β-oxidation	NC	affy
ech-5	enoyl-CoA hydratase	fatty acid β-oxidation	NC	affy
ech-6	enoyl-CoA hydratase	fatty acid β-oxidation	NC	affy
ech-7	enoyl-CoA hydratase	fatty acid β-oxidation	1.46	qPCR
F54C8.1	3-hydroxyacyl-CoA dehydrogenase	fatty acid β-oxidation	NC	affy
B0272.3	3-hydroxyacyl-CoA dehydrogenase	fatty acid β-oxidation	NC	qPCR
T08B2.7	enoyl-CoA hydratase / 3-hydroxyacyl-CoA dehydrogenase	fatty acid β-oxidation	NC	affy
hacd-1	3-hydroxyacyl-CoA dehydrogenase	fatty acid β-oxidation	NC	affy
B0303.3	3-ketoacyl-CoA thiolase	fatty acid β-oxidation	NC	qPCR
T02G5.4	acetoacetyl-CoA thiolase	fatty acid β-oxidation	NC	affy
kat-1	acetoacetyl-CoA thiolase	fatty acid β-oxidation	NC	affy
T02G5.7	acetoacetyl-CoA thiolase	fatty acid β-oxidation	NC	qPCR
gei-7	malate synthase	glyoxylate pathway	0.65	qPCR

Glucose metabolism

Gene ID	Gene Family	Gene Ontology	DA/Veh[a]	Method
F25H5.3	pyruvate kinase	glycolysis	NC	qPCR
ZK593.1	pyruvate kinase	glycolysis	NC	affy
H25P06.1	hexokinase	glycolysis	NC	qPCR
F14B4.2	hexokinase	glycolysis	NC	affy
gpi-1	Glucose -6-phosphate isomerase	glycolysis	NC	qPCR
C50F4.2	6-phosphofructokinase	glycolysis	NC	affy
Y71H10A.1	phosphofructokinase	glycolysis	NC	affy
aldo-2	Fructose-biphosphate aldolase	glycolysis	NC	affy
aldo-1	Fructose-biphosphate aldolase	glycolysis	NC	affy
pgk-1	3-phosphoglycerate kinase	glycolysis	NC	affy
tpi-1	triosephosphate isomerase	glycolysis	NC	affy
T05H10.6	pyruvate dehydrogenase	glycolysis	NC	affy

C04C3.3	pyruvate dehydrogenase	glycolysis	NC	affy
C30H6.7	pyruvate dehydrogenase	glycolysis	NC	affy
F23B12.5	pyruvate dehydrogenase	glycolysis	NC	affy
Idh-1	Lactate DeHydrogenase	glycolysis	NC	affy
R11A5.4	phosphoenolpyruvate carboxykinase (PEPCK)	gluconeogenesis	NC	affy
W05G11.6	phosphoenolpyruvate carboxykinase (PEPCK)	gluconeogenesis	NC	affy
fbp-1	fructose 1,6-bisphosphatase	gluconeogenesis	NC	affy
gpd-2	glyceraldehyde-3-phosphate dehydrogenases	glycolysis/gluconeogenesis	NC	affy
gpd-3	glyceraldehyde-3-phosphate dehydrogenases	glycolysis/gluconeogenesis	NC	affy
gpd-4	glyceraldehyde-3-phosphate dehydrogenases	glycolysis/gluconeogenesis	NC	affy
F57B10.3	phosphoglycerate mutase	glycolysis/gluconeogenesis	NC	affy
C01B4.6	aldose 1-epimerase	glycolysis/gluconeogenesis	NC	affy
enol-1	phosphopyruvate dehydratase	glycolysis/gluconeogenesis	NC	affy
K08E3.5	UDP-glucose pyrophosphorylase	glycogenesis	NC	qPCR
gsy-1	glycogen synthase	glycogenesis	NC	affy
Y50D7A.3	Phosphorylase kinase gamma subunit	glycogenesis	NC	affy
R05F9.6	phosphoglucomutase	glycogenolysis/glycogenesis	NC	affy
Y43F4B.5	phosphoglucomutase	glycogenolysis/glycogenesis	NC	affy
R06A4.8	glycogen debranching enzyme	glycogenolysis	NC	affy
gsk-3	Glycogen synthase kinase-3	glycogenolysis	NC	affy

DAF-12 signaling pathway

Gene ID	Gene Family	Gene Ontology	DA/Veh[a]	Method
daf-28	insulin/IGF-I	insulin/IGF-I signaling	0.19	qPCR
daf-7	TGF-b	TGF-b signaling	0.59	qPCR
daf-12	LXR, VDR, FXR	Nuclear Receptor	0.37	qPCR
daf-9	CYP450	steroid hormone metabolism	0.58	qPCR
strm-1	SAM-dependent methyltransferases	steroid hormone metabolism	3.14	qPCR

TCA cycle

Gene ID	Gene Family	Gene Ontology	DA/Veh[a]	Method
Y48B6A.12	malate dehydrogenase	TCA	NC	qPCR
F36A2.3	malate dehydrogenase	TCA	NC	qPCR
W02F12.5	2-oxoglutarate dehydrogenase	TCA	NC	qPCR
T22B11.5	2-oxoglutarate dehydrogenase	TCA	NC	qPCR
sdha-1	succinate dehydrigenase	TCA	NC	qPCR
LLC1.3	dihydrolipoamide dehydrogenase	TCA	NC	qPCR
aco-1	aconitase	TCA	1.80	qPCR
aco-2	aconitase	TCA	NC	qPCR

a, fold changes in expression in *din-1daf-9* mutants, upon DAF-12 activation; NC, no change.

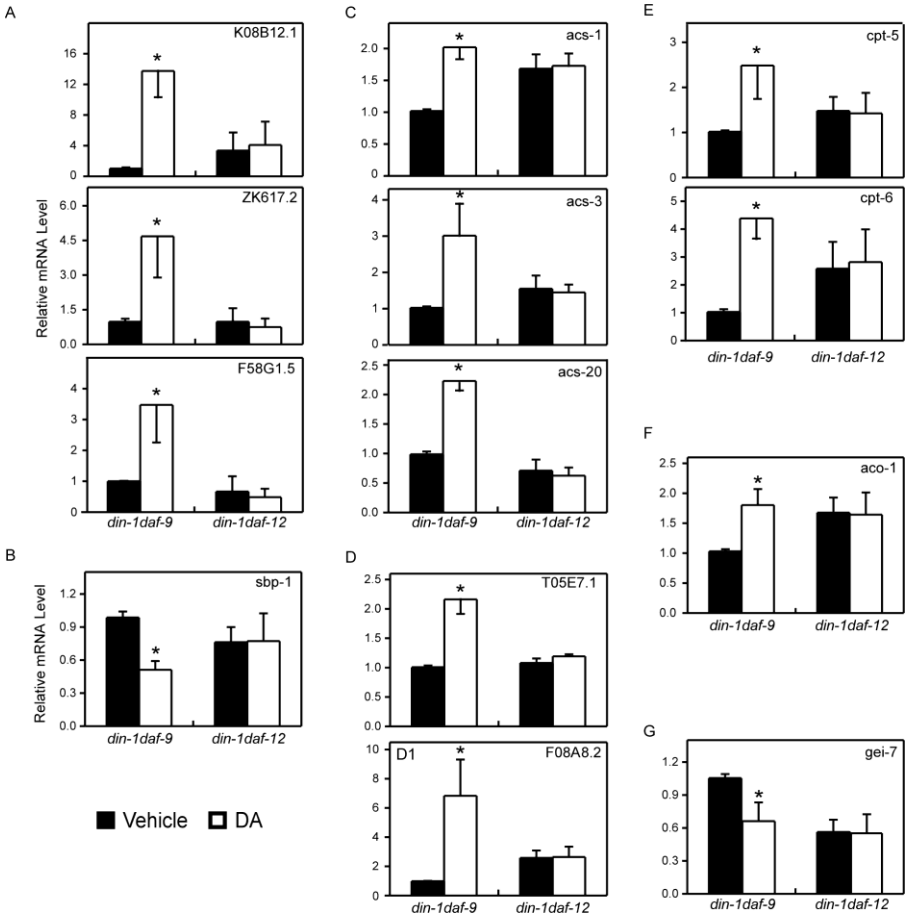

Figure 1-4. DAF-12 Regulates Lipid Metabolic Genes

(A-B) Expression of metabolic genes that regulate lipid storage in the indicated mutant worms treated with vehicle control or DA. K08B12.1, ZK617.2 and F58G1.5 are triglyceride lipases (A) and *sbp-1* is the homolog of *SREBP-1c* in *C. elegans* (B). (C) Expression of metabolic genes that catalyze fatty acid activation in the indicated mutant worms treated with vehicle control or DA. *acs* is acyl-CoA synthetase. (D-E) Expression of metabolic genes that are involved in peroxisomal (D) or mitochondrial β-oxidation (E), in the indicated mutant worms treated with vehicle control or DA. (F) Expression of *aco-1*, an aconitase, in the indicated mutant worms treated with vehicle control or DA. (G) Expression of *gei-7*, a malate synthase, in the indicated mutant worms treated with vehicle control or DA. Data represent at least three independent experiments.

1.2.2 DAF-12 Regulates Lipid Metabolic Genes

To provide insight into the molecular basis for DAF-12's effect on energy metabolism, we implemented a strategy of DNA microarray followed by qPCR verification to uncover the metabolic genes that are under the control of DAF-12 (Table 1-1). We found that DAF-12 preferentially regulated genes that are involved in fat metabolic processes, including lipogenesis and lipolysis, as well as fatty acid activation, desaturation, and β-oxidation. In contrast, genes responsible for glucose metabolism were not affected, which is consistent with the notion that DAF-12's effect on reproductive growth is not mediated by these metabolic processes. Moreover, DAF-12 did not impose a global effect on all members of the same family, showing, instead, a specific regulatory profile on certain metabolic genes (Table 1-1).

Fatty acids may originate directly from the diet or from stored triglycerides via a mobilizing process that is catalyzed by TG lipases (Figure 1-3A). In *din-1daf-9* worms treated by Δ^7-DA, we observed elevated expression of TG lipases (Figure 1-4A), indicating that an augmentation in fatty acid mobilization is occurring. Meanwhile, *sbp-1*, the homolog of *SREBP-1c* that is required for lipid deposition in *C. elegans*, was also down-regulated (Figure 1-4B). Collectively, this manner of gene regulation indicated that DAF-12 activation could provide more fatty acids for aerobic catabolism, by increasing mobilization and reduced synthesis of stored lipids, while leaving dietary intake unaffected (Figure 1-3C).

Before undergoing oxidative degradation, free fatty acids must be esterified to coenzyme A, a process that is facilitated by a family of enzymes called acyl-CoA synthases (ACS) (Figure 1-3A). When challenged with Δ^7-DA, *din-1daf-9* worms

exhibited enhanced expression of several genes encoding ACS, including *acs-1*, *acs-3*, and *acs-20* (Figure 1-4C). Furthermore, enzymes that are involved in peroxisomal β-oxidation, such as acyl-CoA oxidase (F08A8.2) and long chain acyl-CoA thioesterase (T05E7.1), were also upregulated (Figure 1-4D). In particular, *cpt-5* and *cpt-6*, two homologous genes encoding carnitine palmitoyltransferases (CPT), which mediate the translocation of fatty acyl-CoAs into mitochondria and act as the rate-limiting enzyme for mitochondrial β-oxidation, were induced by DAF-12 activation (Figure 1-4E). Finally, expression of an aconitase *aco-1*, an enzyme involved in TCA cycle, was increased as well (Figure 1-4F). In opposition, the malate synthase *gei-7*, which is involved in the glyoxylate pathway and is required for anaerobic lipid catabolism, was suppressed by DAF-12 (Figure 1-4G). These effects of DAF-12 cooperatively facilitated the flow of fatty acids into aerobic catabolic pathways, which are capable of producing energy efficiently for the rapid reproductive growth .

Also under the regulation of DAF-12 was the hormone signaling network that is upstream of the nuclear receptor itself. Molecules that increase DA synthesis, such as DAF-28 and DAF-7 (insulin/IGF-I and TGF-β homologs, respectively), and DAF-9 (the DA synthetic enzyme), were suppressed by DAF-12 (Figure 1-5A), whereas STRM-1, the methyl transferase that quenches DAF-12 signaling (Hannich et al., 2009), was up-regulated (Figure 1-5B). Also, DAF-12 down-regulated itself as well (Figure 1-5C). These data clearly delineate a canonical negative feedback loop, which has been seen in many other nuclear receptor signaling pathways, especially those involved in metabolic homeostasis.

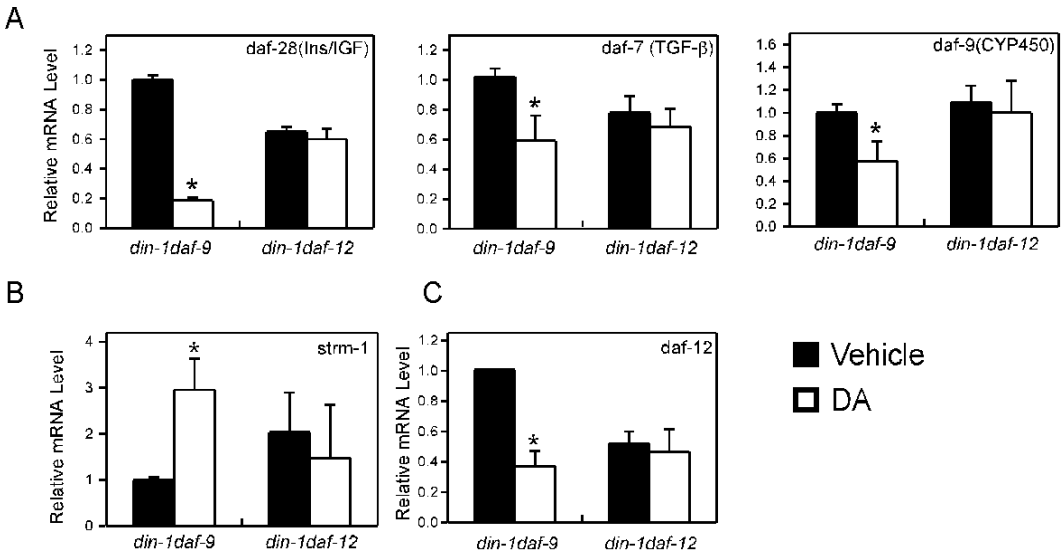

Figure 1-5. Negative Feeding Back Regulation of DAF-12 Signaling Pathway

(A) Expression of the genes *daf-2*, *daf-7* and *daf-9*, which increase DA synthesis, in the indicated mutant worms treated with vehicle or DA. (B) Expression of strm-1 which suppresses DA synthesis, in the indicated mutant worms treated by vehicle or DA. (C) Expression of DAF-12 in the indicated mutant worms treated by vehicle or DA. Data represent at least three independent experiments.

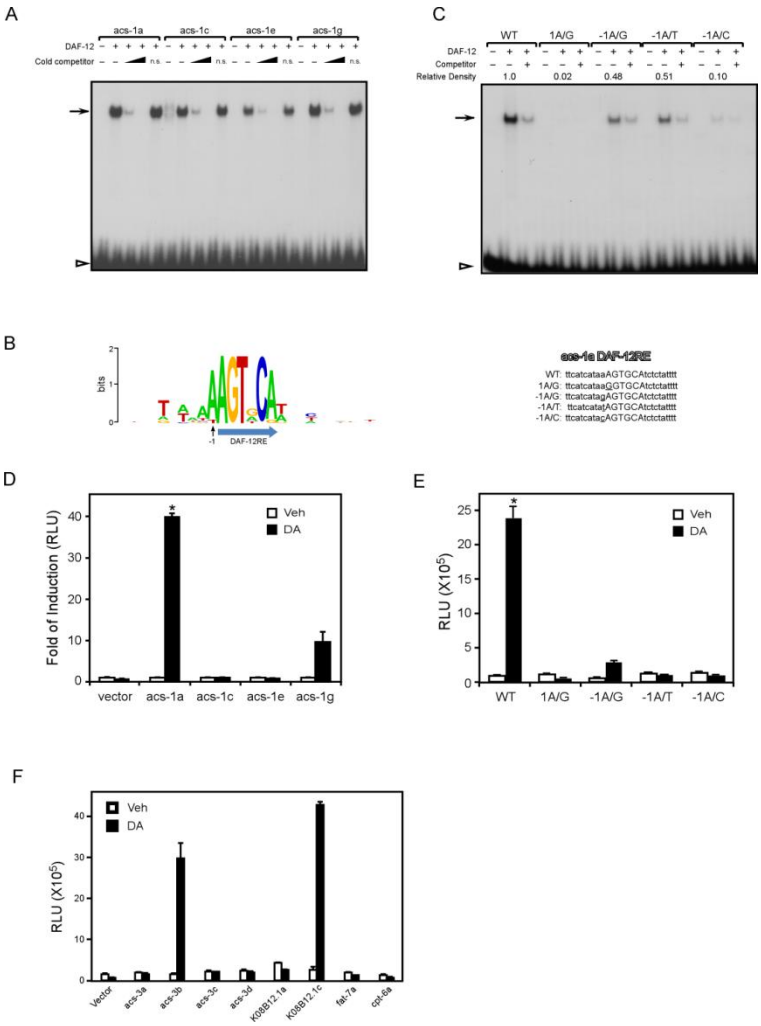

Figure 1-6. Identification of DAF-12 Response Elements in the Regulatory Genome Region of Lipid Metabolic Genes

(A) EMSA detection of DAF-12 binding to *acs-1* DAF-12REs. acs-1a, c, e, g, indicates different DAF-12REs within the *acs-1* gene. Arrow, DAF-12-bound probes; arrow head, free probes. (B) Consensus sequence of DAF-12REs to which DAF-12 binds (left panel) and the sequences of acs-1a DAF-12RE mutants (right panel). (C) EMSA detection of DAF-12 binding to the mutated *acs-1* DAF-12REs. (D) Cell-based reporter assay to detect the transcriptional activities of *acs-1* DAF-12REs. (E) Cell-based reporter assay to detect the transcriptional activities of mutant acs-1as. (F) Cell-based reporter assay to detect the transcriptional activities of DAF-12REs from the gene regulatory regions of *acs-3*, K08B12.1, *fat-7*, and *cpt-6*. Experiments were repeated at least three times with similar results.

Table 1-2. Genomic sequences that contains potential DAF-12REs

DAF-12 REs	Sequence	Target Gene	Position [a]	EMSA Binding?[b]	Reporter Activity? [c]
acs-1a	ttcatcataaAGTGCAtctctatttt	*acs-1*	-2230	Yes	Yes
acs-1b	tggtttagtcAGTTCAgaaatgaacc	*acs-1*	-1492	No	NA
acs-1c	gttggaaaaaAGTACAttaaataatt	*acs-1*	-903	Yes	No
acs-1d	atgtataattAGGACAtctgttctac	*acs-1*	270	No	NA
acs-1e	aagtttttaAGTGCAtttttattgt	*acs-1*	1499	Yes	No
acs-1f	tcccgatcttAGTTCAgatgactctt	*acs-1*	1927	No	NA
acs-1g	aaaatcacaaAGTGCAaaatgaaaaa	*acs-1*	2511	Yes	Yes
acs-1h	ctatagtctcAGTACAttctagccct	*acs-1*	2659	No	NA
acs-1i	ctttacaaacAGTACAaacttttttt	*acs-1*	2911	No	NA
acs-1DR4	aagataacgcAGTGCAaatgAGTGGAattgaaaaaa	*acs-1*	3048	No	NA
acs-3a	caattaaaatAGTGCAtacaatagct	*acs-3*	-4522	Yes	No
acs-3b	ctttttataaAGTACAtttcctcatt	*acs-3*	-3496	Yes	Yes
acs-3c	tgaaggtaaaAGTGCAttatggttag	*acs-3*	-3079	Yes	No
acs-3d	gtactgtaaaAGTTCAacaaagcgtt	*acs-3*	-2803	Yes	No
cpt-6a	attgtttacaAGTGCAgccccagtat	*cpt-6*	-2052	Yes	No
cpt-6IR9	ataattttccAGTGCGtttttaagcTGAACTttcatttgaa	*cpt-6*	-1516	No	NA
cpt-6ER10	aggtaattttAGCACTggttttaaacAGTACTcccaattctt	*cpt-6*	-1193	No	NA
K08B12.1a	cgatattgtaAGTACAaacctcttcc	K08B12.1	-2299	Yes	No
K08B12.1b	gtgcacaatgAGTACAagagacagtc	K08B12.1	-1695	No	NA
K08B12.1c	acgcacaagaAGTACAaagttgatga	K08B12.1	-1592	Yes	Yes
K08B12.1d	gatgaggggggAGGGCAccagatatga	K08B12.1	-1563	No	NA
K08B12.1e	tcgacgctacAGTACTcatgtaaagt	K08B12.1	-1105	No	NA
K08B12.1f	tccgtccatcAGTGCTtccagatgcc	K08B12.1	-431	No	NA
fat-7a	ttggtctgaaAGTTCAagacggagag	*fat-7*	-1918	Yes	No
fat-7b	aacgattcggAGGGCAaagagtcttc	*fat-7*	-240	No	NA
T05E7.1a	agaatgggttAGTACAatataatcta	T05E7.1	-1994	No	NA
T05E7.1b	catttgaagaAGTGCGatctccgatt	T05E7.1	-1892	No	NA
T05E7.1c	aatgttaggtAGTTCAttacagcgtc	T05E7.1	-921	No	NA
T05E7.1ER2	ggttgcacgtTGTCCTagAGTTCAaacaacttac	T05E7.1	-1962	No	NA

a, determined in reference to translational start point
b, DAF-12 binding of REs as detected by EMSA
c, Induction of downstream gene transcription in response to DA , as tested by cell-based reporter assay. NA, data are not available.

1.2.3 Identification of DAF-12 Response Elements that Control Lipid Metabolic Gene Transcription

As transcription factors, nuclear receptors can directly bind short sequences of genomic DNA called response elements in order to regulate transcription of target genes. We therefore addressed the question of whether the lipid metabolic genes are direct targets of DAF-12 by indentifying DAF-12 response elements (DAF-12REs) in the putative target gene promoters. We selected six DA-induced genes as representatives for those involved in multiple fat metabolic processes, including lipolysis, fatty acid activation, desaturation, and β-oxidation.

An initial bioinformatic approach using previously reported 6-bp motifs identified twenty nine putative DAF-12REs located within the introns and 5kb promoters of the chosen genes (Shostak et al., 2004). Based on these, we designed individual oligonucleotide probes that contained the DAF-12REs and 10 bp of flanking genomic sequences (Table 1-2). We then tested whether DAF-12 could bind these probes by electrophoresis mobility shift assays (EMSA). We found that twelve of these probes, which corresponded to five of the chosen genes, could physically interact with DAF-12 (Table 1-2). In the case of the *acs-1* gene, DAF-12 specifically bound to four out of ten putative DAF-12REs, named acs-1a, c, e, g (Figure 1-6A). The fact that DAF-12-DNA binding was observed only for a subset of putative response elements indicated that additional requirements for the recognition existed. To illustrate these determinants, we performed a sequence alignment of the twelve probes that interacted with the DAF-12 protein. We found that the nucleotide immediately preceding the DAF-12REs displayed remarkable conservation and was dominantly occupied by adenosine (Figure 1-6B). In

contrast, this site showed no conservation in those probes that did not interact with DAF-12 (Figure 1-7), indicating that this nucleotide was important for DAF-12 binding. As expected, mutating this nucleotide reduced the binding of the response element with DAF-12 (Figure 1-6C). Next, to test whether the DAF-12REs could induce downstream gene transcription, we employed a convenient, mammalian cell-based reporter assay that is designed specifically for this purpose. As shown in Figure 1-6D, a single copy of the DAF-12RE (i.e. acs-1a or acs-1g) was sufficient to drive robust reporter gene expression in response to Δ^7-DA. This DA-responsiveness, however, was abolished by interfering with DAF-12 binding to its response element (Figure 1-4E). These results indicated that acs-1 is a direct target gene of DAF-12.

Using a similar strategy, we identified DA-responsive DAF-12REs in the promoters of the other metabolic genes, including *acs-3*, another ACS, and K08B12.1, which is a triglyceride lipase (Figure 1-6F). It is also worth mentioning that we did not

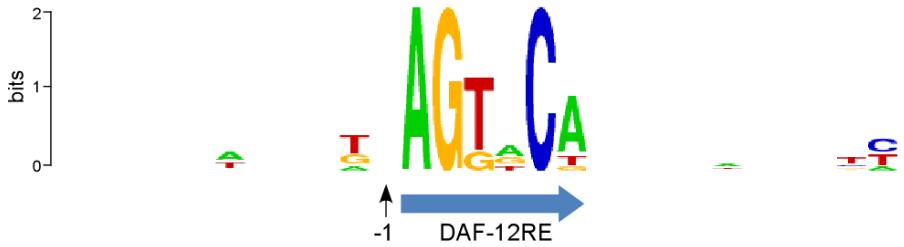

Figure 1-7. Consensus sequence of DAF-12 response elements that do not interact with DAF-12.

Sequences from DAF-12 response elements that bind with DAF-12 are aligned and consensus sequence is generated by using WebLogo (http://weblogo.berkeley.edu/). Arrow, 6-bp DAF-12 response element; arrow, the nucleotide before DAF-12RE, which is conserved in DAF-12RE that is able to bind with DAF-12.

find DA-responsive DAF-12REs within the other three representative genes (cpt-6, T08E7.1 and fat-7), although the elements from the cpt-6 and fat-7 promoters showed strong interaction with DAF-12 *in vitro* (Table 1-2). These data suggested a DAF-12-DNA interaction was not sufficient for this nuclear receptor to induce downstream target genes and additional structural determinants and coactivator/corepressor might be further studied.

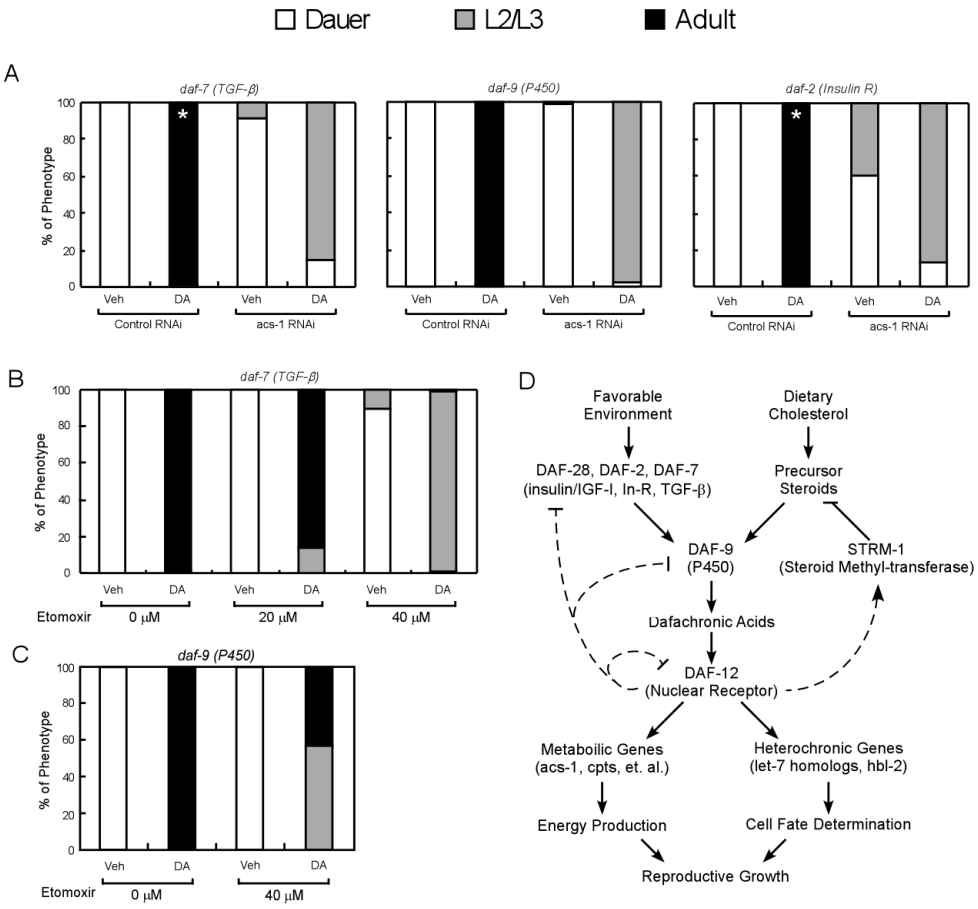

Figure 1-8. Aerobic catabolism of fatty acids is required for DAF-12-induced reproductive growth in *C. elegans*

(A) Effect of *acs-1* RNAi on DA-induced reproductive growth in *daf-7*, *daf-2* and *daf-9* mutant worms. (B-C) Effect of CPT inhibition on DA-induced reproductive growth in *daf-7* (B) and *daf-9* (C) mutant worms. Eto, etomoxir, a CPT inhibitor. (D) Summary of the signaling pathways controlling larval development in *C. elegans*. Data were collected from three independent experiments and combined for analysis. *, $p<0.01$, by χ^2-test, compared with the vehicle treated worms.

1.2.4 Reproductive Growth in *C. elegans* Requires DAF-12-Stimulated Lipid Catabolism

Previously, we demonstrated that DAF-12 activation could commit *C. elegans* to reproductive growth, bypassing dauer diapause (Motola et al., 2006; Sharma et al., 2009). As a result, DAs could induce normal reproductive growth to fertile adulthood in the mutants with deficiencies in transducing environment signals to DAF-12 (i.e. *daf-2*, *daf-7*, and *daf-9* mutants), which would otherwise display constitutive dauer formation (*daf-c*). These mutants therefore provided us with convenient tools to evaluate the effect of DAF-12-induced lipid catabolism on *C. elegans* reproductive growth.

The initial step in fatty acid utilization is to esterify the carboxyl group with a coenzyme A, a reaction catalyzed by the enzyme ACS. We therefore fed the *daf-c* mutants RNAi against acs-1, an ACS that was directly induced by DAF-12, to interfere with the DAF-12-mediated lipid catabolism. Although reproductive growth was completely rescued by Δ^7-DA in all three mutants fed with control RNAi, no fertile adult was obtained when acs-1 RNAi was fed to these worms. Instead, they arrested at the L2- or L3-stage, even in the presence of Δ^7-DA (Figure 1-8A). Interestingly, however, this Δ^7-DA treatment was sufficient to suppress dauer formation that occurred in the vehicle treated worms, indicating that whereas the DAF-12-promoted lipid catabolism was required to support complete reproductive growth, it was dispensable to merely commit *C. elegans* to this developmental track.

To be utilized aerobically, fatty acids need to be transported into mitochondria, where mitochondriąl β-oxidation and further energy producing processes occur. This step, which is rate-limiting for lipid catabolism, is catalyzed by the enzyme CPT, whose

C. elegans homologs (*cpt-5* and *cpt-6*) were induced by DAF-12 (Figure 1-8B). By administrating etomoxir, a specific CPT inhibitor, we could abolish the adulthood rescue of reproductive growth by Δ^7-DA in *daf-7* mutants. Also, as in the RNAi experiments, the DA-treated worms arrested at the L2/L3-stage (Figure 1-8B). Similar results were also obtained with *daf-9* mutants (Figure 1-8C), except that the rescue effect of DA was impaired in a relatively smaller population (57% in *daf-9 versus* 98% in *daf-7*). However, unlike in the *daf-7* and *daf-9* worms, etomoxir failed to block the reproductive growth in the DA-treated *daf-2* mutants, wherein it just retarded the timing of progression to adulthood (data not shown). This indicated that complementary energy metabolic pathways are engaged in this insulin deficient mutant (see discussion).

1.3 DISCUSSION

1.3.1 DAF-12 Coordinates Energy Metabolism and Larval Development in *C. elegans*

Appropriate nutrient responses are fundamental for animals to maintain metabolic homeostasis, maintain good health, and reproduce successfully. Based on the availability of the nutrient supply, the size of the animal population, and the ambient temperature (which affects the expansion rate of the population), *C. elegans* evaluates the environmental nutrition status, and accordingly decides to execute reproductive growth or arrest at dauer diapause, strategically maximizing its reproductive value. Associated with the developmental alternatives are distinct energy metabolic styles: whereas dauers engage in very slow metabolism to meet their minimal energy requirements and survive for an extended lifespan, larvae in reproductive growth actively produce energy by invoking energetically-efficient aerobic catabolism (Riddle and Albert, 1997). In this study, we found that the nuclear receptor DAF-12, which was previously reported to induce stage-specific cell fate changes for reproductive growth (Bethke et al., 2009; Hammell et al., 2009), also determined the style of energy metabolism that supports this development. In the presence of its ligands, DAF-12 regulates various lipid metabolic genes, which cooperatively promote the aerobic catabolism of fatty acids as well as *C. elegans* reproductive growth. During dauer diapause, however, DAs are absent, and the gene regulation is missing, which allows conservative, anaerobic energy metabolism. In conclusion, our work has uncovered a DAF-12-regulated metabolic network that coordinates *C. elegans* energy metabolism for its larval development in response to environmental nutritional status (Figure 1-8D). Furthermore, our findings support the

notion that conserved steroid hormone signaling pathways governed by DAF-12 and its homologs (LXR and DHR96) modulate the animal's nutrient responses (Figure 1-2A).

The insulin/IGF-I signaling pathway is conserved and controls nutrient responses in animals. In *C. elegan*s, DAF-12 and the FOXO transcription factor DAF-16 are two outputs of this nutrient responsive signaling pathway, as indicated by epistasis analysis. Whereas DAF-12 is active in reproductively growing larvae in the fed state, DAF-16 is stimulated when the worm is in dauer diapause or undergoing starvation (Henderson and Johnson, 2001). In response to a scarcity of nutrients, DAF-16 enhances anaerobic lipid catabolism, which converts lipid storage to glucose for utilization, by inducing glyoxylate and gluconeogenic genes in *C. elegans* (Murphy et al., 2003). Mirroring this, our findings indentifying DAF-12 as an activator of aerobic lipid catabolism reveals the mechanisms through which energy metabolism is adjusted to adapt to the abundance of nutrients. Although they have directly opposing effects on dauer regulation, DAF-12 and DAF-16 seem to operate their metabolic functions independently. As a matter of fact, the increased DAF-16 activity in the *daf-2* mutants enables the worms to survive the inhibition against the DAF-12-controlled aerobic catabolism of lipids (data not shown) .

Table 1-3. Metabolic Genes that are Regulated either by DAF-12 or by NHR-49

Gene ID	Gene Ontology	DAF-12[a]	NHR-49[b]
FASN-1	fatty acid synthesis	2.92	1.00
fat-5	fatty acid synthesis	0.72	161.01
fat-6	fatty acid synthesis	1.00	3.46
fat-7	fatty acid synthesis	12.85	97.51
Y54E5A.1	fatty acid synthesis	1.00	0.45
cpt-1	β-oxidation	0.78	1.00
cpt-5	β-oxidation	2.49	55.72
acs-1	fatty acid transport	2.02	1.00
acs-2	fatty acid transport	0.38	110.39
acs-4	fatty acid transport	0.63	1.00
lbp-5	fatty acid binding & transport	0.45	1.00
lbp-7	fatty acid binding & transport	0.48	0.67
lbp-8	fatty acid binding & transport	0.31	3.88
F08A8.2	β-oxidation	6.83	1.00
F59F4.1	β-oxidation	0.65	1.00
C48B4.1	β-oxidation	0.46	0.55
ech-1	β-oxidation	1.00	23.98
ech-7	β-oxidation	1.46	1.00
ech-9	β-oxidation	0.54	0.05
aco-1	TCA, glyoxylate pathway	1.80	1.00
gei-7	glyoxylate pathway	0.65	3.71
sdha-1	TCA, glyoxylate pathway	1.00	1.64

a, fold changes in expression in *din-1daf-9* mutants upon DAF-12 activation
b, fold changes in expression in wild type C. elegans versus nhr-49 mutants; results were calculated according to Van Gilst et al., 2005a.

1.3.2 Distinct Energy Metabolic Networks are Controlled by Nematode Nuclear Receptors

Like DAF-12, the nuclear receptor NHR-49, which is the nematode homolog of hepatic nuclear factor-4 (HNF-4), promotes lipid catabolism in *C. elegans* (Van Gilst et al., 2005a; Van Gilst et al., 2005b). However, NHR-49 only provokes the metabolic process in response to food deprivation, which allows the worm to survive nutrient starvation. As a result, the worm can enter an adult reproductive diapause (ARD) and reproductive longevity is extended (Angelo and Van Gilst, 2009). On the level of gene expression, DAF-12 and NHR-49 produce different effects on lipid metabolic genes (Table 1-3). In particular, these two fat modulators selectively regulate different paralogous members of the same gene family. For instance, *acs-2*, a member of the ACS gene family that is dramatically induced by NHR-49 in response to nutrient starvation, is suppressed by the activation of DAF-12, whereas its paralog, *acs-1*, is stimulated by DAF-12, and remains intact regardless of the presence of NHR-49. DAF-12 and NHR-49 also have common metabolic targets, as evidenced by genes such as *fat-7* and *lbp-1* that are regulated in the same direction by the two nuclear receptors (Table 1-3). These facts clearly delineate two overlapping but distinct metabolic networks that are regulated by DAF-12 and NHR-49 in order to control aerobic and anaerobic energy metabolism, respectively .

CHAPTER TWO

Identification of the Nuclear Receptor DAF-12 as a Therapeutic Target in Human Parasitic Nematodes

2.1 INTRODUCTION

Nematode parasitism is a worldwide health problem resulting in symptoms from malnutrition to death in over 1 billion people (Hotez et al., 2006; Jasmer et al., 2003). One of the most problematic parasites, *Strongyloides stercoralis*, is estimated to infect 100-200 million people. Primary infections are often asymptomatic and clinically silent in immunocompetent individuals. However, once the immune system is compromised (e.g., by corticosteroid therapy), the parasite establishes autoinfection cycles that result in a frequently fatal disseminated strongyloidiasis (Igra-Siegman et al., 1981; Viney and Lok, 2007). Hookworms *(Ancylostoma* and *Necator spp.)* are other parasitic nematodes that affect >1 billion people and are the dominant cause of iron-deficient anemia worldwide (Hotez et al., 2006). Oral administration of anthelmintics such as benzimidazoles (microtuble toxins) and ivermectin (a neurotoxin) is currently the preferred treatment for nematode infections (Muller, 2002). However, no reliable options exist for treating the more severe form of disseminated strongyloidiasis (Fox, 2006). Moreover, resistance to the anthelmintics has become widespread in animal parasites and is beginning to occur in human parasites (Hotez et al., 2006; Kaplan, 2004). Therefore, studying the mechanisms that govern nematode life cycles is an attractive approach to identifying new therapeutic targets.

Infection of hosts by parasitic nematodes is mediated by infective larvae, which in *S. stercoralis* and hookworm are the third stage or L3 larvae (iL3) (Muller, 2002; Viney and Lok, 2007). Interestingly, iL3 larvae resemble the dauer larvae of the free-living nematode *Caenorhabditis elegans (C. elegans)* in that they are all non-feeding, developmentally-arrested, dormant filariform larvae with a sealed buccal capsule and thickened body wall cuticle, enabling them to survive environmental challenges (Hotez et al., 1993). Like *C. elegans* dauer larvae, iL3s recover from their arrested development once they enter a proper environment (i.e., their respective hosts) (Hawdon and Schad, 1990). To date the molecular mechanisms controlling the recovery of iL3 parasites are poorly understood.

In *C. elegans*, dauer diapause is controlled by endocrine signals in response to environmental cues. In favorable environments, reproductive development requires an insulin/IGF-I (II-S) and TGFβ signaling network that converges on a downstream steroid hormone/nuclear receptor signaling pathway mediated by the nuclear receptor, DAF-12 (Antebi, 2006). Previously, we have shown steroid hormones named dafachronic acids (DAs), which are *de novo* synthesized from dietary sterols by the cytochrome P450 DAF-9, activate DAF-12 and promote dauer recovery in *C. elegans* (Motola et al., 2006). For parasitic nematodes, it has also been reported that the induction by the host of the II-S pathway is essential for iL3 recovery (Brand and Hawdon, 2004; Tissenbaum et al., 2000). Based on the similarities between free-living and parasitic worms, we hypothesized that the steroid hormone/nuclear receptor signal (i.e., DA/DAF-12) would also be conserved and control the dauer-like iL3 diapause in parasitic nematodes (Figure 3-1*A*). In the present study, we identified the DAF-12 orthologs in several parasitic

species and showed these receptors respond to DAs. Remarkably, administration of DAs caused a significant proportion of worms in the post-free-living generation of *S. stercoralis* to form supernumerary free-living but unviable L4s. There was a corresponding and profound reduction in the population of the pathogenic *S. stercoralis* iL3, suggesting that these compounds or their congeners might be used as a new class of drugs for treatment of disseminated strongyloidiasis. Finally, we report the X-ray crystal structure of the DAF-12 ligand-binding domain for *S. stercoralis*, which is the first structure described for one of the hundreds of nuclear receptors found in nematodes and provides a powerful new tool for drug development.

2.2 RESULTS

2.2.1 DAF-12 Homologues in Parasitic Nematodes

Based on the hypothesis that iL3 and dauer represent homologous stages in nematode development (Figure 2-1*A*), we investigated whether iL3 diapause is regulated by a DAF-12-like nuclear receptor. We analyzed the parasitic nematode genome database (www.nematode.net) and subsequently cloned full-length cDNAs encoding DAF-12 orthologs from *S. stercoralis* (Siddiqui et al., 2000) (ssDAF-12) and the dog hookworm *Ancylostoma caninum* (acDAF-12); as well as partial cDNAs encoding a.a. 378-686 of the pan-specific hookworm *Ancylostoma ceylanicum* DAF-12 ligand-binding domain *(*aceDAF-12) and a.a. 274-686 of the human hookworm *Necator americanus* (naDAF-12). These cDNAs shared significant identities with *C. elegans* DAF-12 (ceDAF-12) in their corresponding DNA and ligand-binding domains (Figure. 2-1*B* and Figure 2-2). Notably, all of the parasitic DAF-12s exist in iL3 cDNA libraries, indicating their physiological expression in the dauer-like larvae.

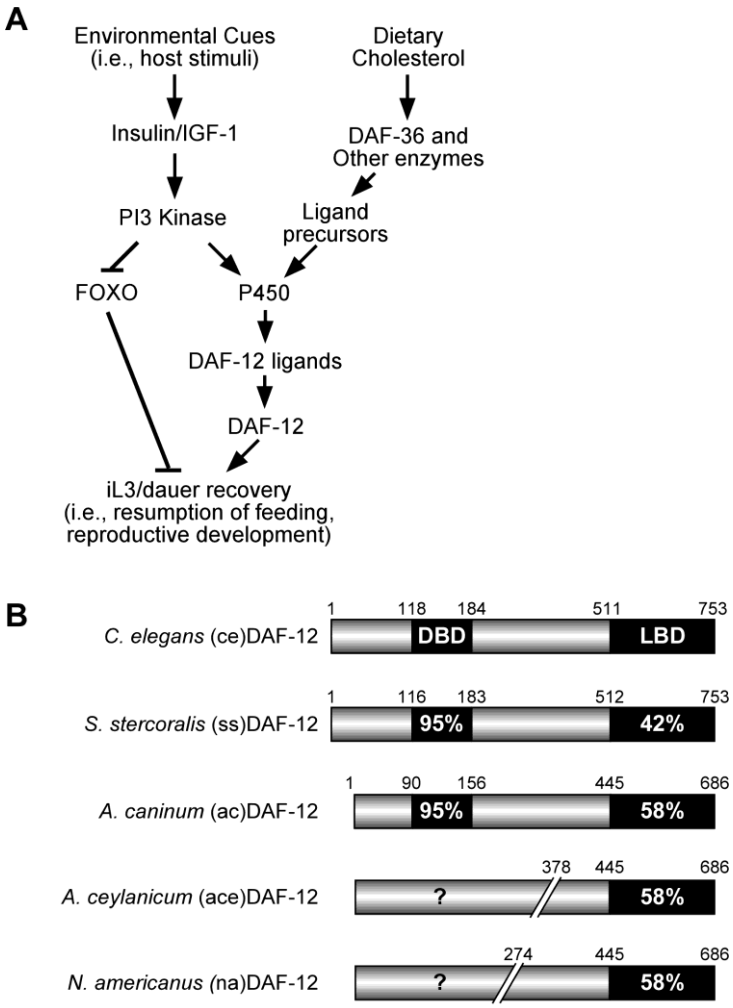

Figure 2-1. Conserved nuclear receptor signaling pathway controls dauer/iL3 diapause. (*A*) Schematic for signaling pathways that control dauer/iL3 diapause. (*B*) Sequence similarities of DAF-12 homologues in parasitic nematodes. DAF-12 amino acid positions in the partial *A. ceylanicum* and *N. americanus* cDNA clones were assigned according to their homologous positions in *A. caninum*.

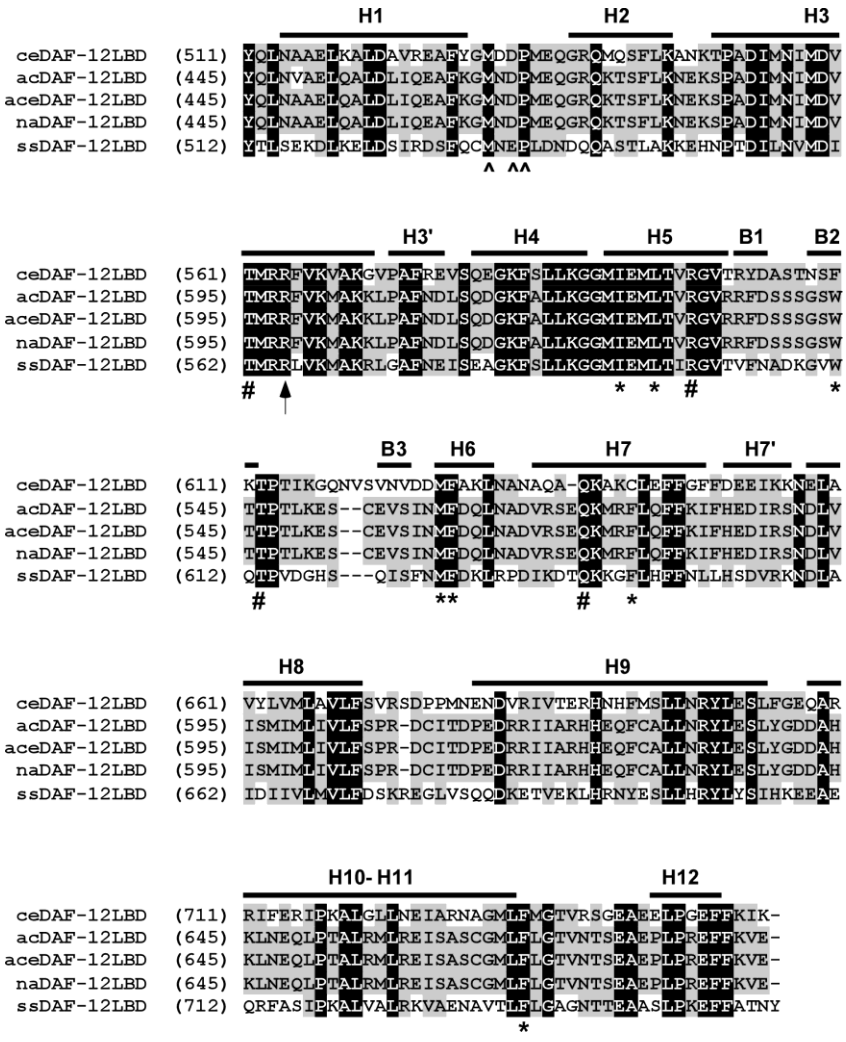

Figure 2-2. Sequence comparison of nematode DAF-12 ligand binding domains. DAF-12 secondary structure alignments for *C. elegans* (ce), *A. caninum* (ac), *A. ceylanicum* (ace), *N. americanus* (na) and *S. stercoralis* (ss) are based the crystal structure of the ssDAF-12 ligand binding domain; H, α-helix, B, β-sheet. *, hydrophobic residues within the ligand-binding pocket; #, residues involved in hydrogen bond formation. Arrow indicates the conserved arginine that donates hydrogen bonds to the main chain oxygen atoms of M532, E534 and P535 (designated by arrowheads), which forms the lid over the ligand-binding pocket.

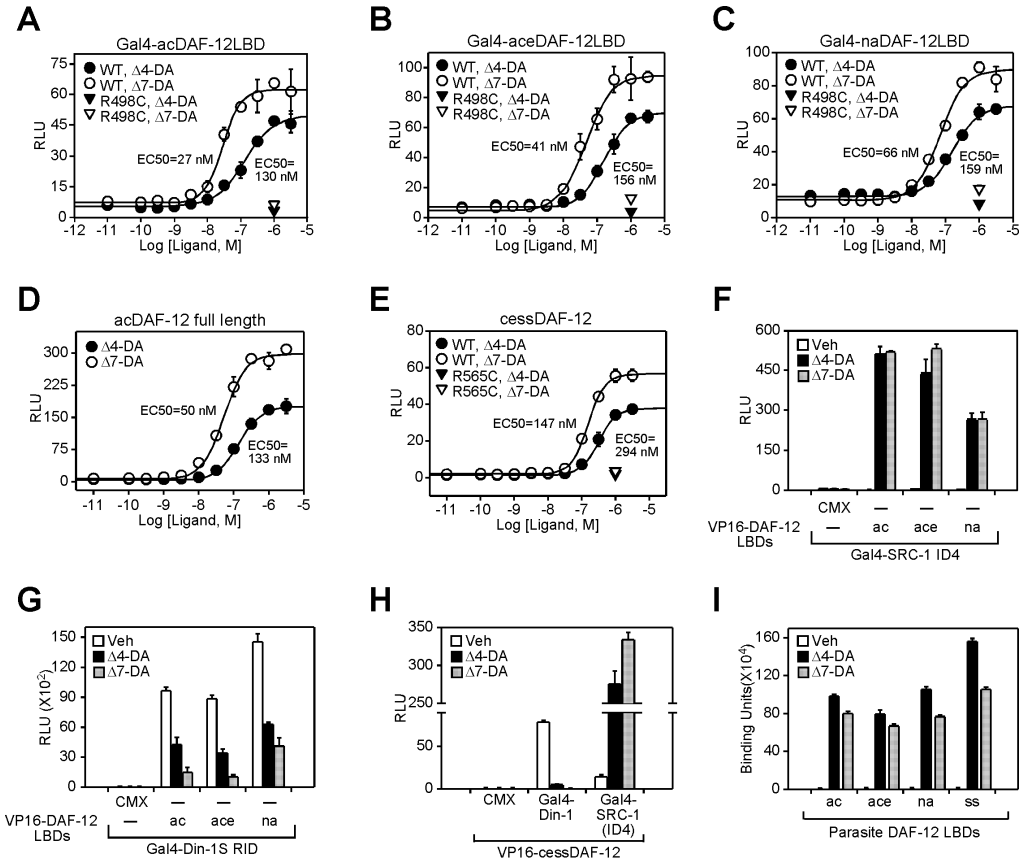

Figure. 2-3. Parasite DAF-12s are activated by dafachronic acids. (*A-E*) Ligand activation of parasite DAF-12 homologues and various ligand binding mutants. (*F-H*) Mammalian 2-hybrid assay for ligand-dependent interaction between parasite DAF-12s and coactivator (SRC-1 ID4) or corepressor (Din-1S RID) interaction domains. Cotransfection assays were performed in HEK293 (*A-C, F-H*) or CV-1 (*D-E*) cells. RLU, relative light units. (*I*) *In vitro* ligand binding of DAs to parasite DAF-12 ligand binding domains as monitored by ligand-induced association of the coactivator LXXLL motif (SRC1-4) with receptor. 1μM of DAs was used in (*F-I*). n=3 ± s.d.

2.2.2 Parasite DAF-12s Are Activated by DAs

We tested whether Δ^4-DA and Δ^7-DA can activate the parasitic DAF-12s in a fashion similar to that observed with *C. elegans* DAF-12 (Motola et al., 2006). We found both Δ^4- and Δ^7-DAs activated Gal4-DAF-12 chimeras when tested in cell-based co-transfection assays (Figure 2-3*A*-*C*). Full-length hookworm acDAF-12 was also able to induce reporter gene expression driven by a promoter containing DAF-12 response elements from the *lit-1* kinase promoter (Shostak et al., 2004), showing that the DNA binding domain is functional (Figure 2-3*D*). Unlike the hookworm DAF-12 constructs, the corresponding *S. stercoralis* DAF-12 does not express well in mammalian cells (data not shown). Therefore, we generated an alternative chimeric expression construct in which the N-terminus of ceDAF-12 (including the DNA binding domain) was fused to the C-terminal ligand-binding domain of ssDAF-12. This hybrid receptor (cessDAF-12) is expressed in cell culture and was capable of robust activation of the *lit-1* kinase reporter by both DAs (Figure 2-3*E*). The EC_{50} for activation of the parasite DAF-12s ranged from 25 nM to 147 nM for Δ^7-DA and 130 nM to 294 nM for Δ^4-DA. This rank order of potency is similar to that observed for ceDAF-12 (Wang et al., 2009). Importantly, activation by DAs could be abolished by mutating the conserved arginine that has been shown to be critical for ligand activation in ceDAF-12 (Figure 2-4*E*). We also employed a mammalian two-hybrid assay to monitor the interaction between the parasite DAF-12s and the receptor interaction domains of the coactivator SRC-1 (SRC1-ID4) and the co-repressor Din-1S (Din-1S RID, identified in Figure 2-4). As predicted,

upon DA treatment the interaction with Din-1S is compromised and that with SRC-1 is induced (Figure 2-3*F-H*).

Finally, to prove that DAs directly bind parasitic DAF-12s, we employed an *in vitro* ligand binding assay that detects agonist-induced interactions between receptor and coactivator peptides containing the LXXLL motif (Motola et al., 2006). We found that both Δ^4-DA and Δ^7-DA bind directly to all parasitic DAF-12s (Figure 2-3*I*), providing unequivocal evidence that DAs act as classical nuclear receptor ligands.

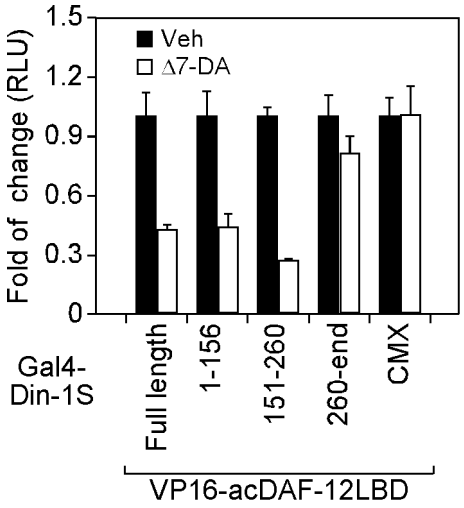

Figure 2-4. Mammalian two-hybrid assay was employed to map the domain within Din-1S that interacts with the acDAF-12 ligand binding domain. Truncations of Din-1S are taken from (Ludewig et al., 2004a). The Gal-4Din-1S (151-260) construct was used for subsequent studies in this work.

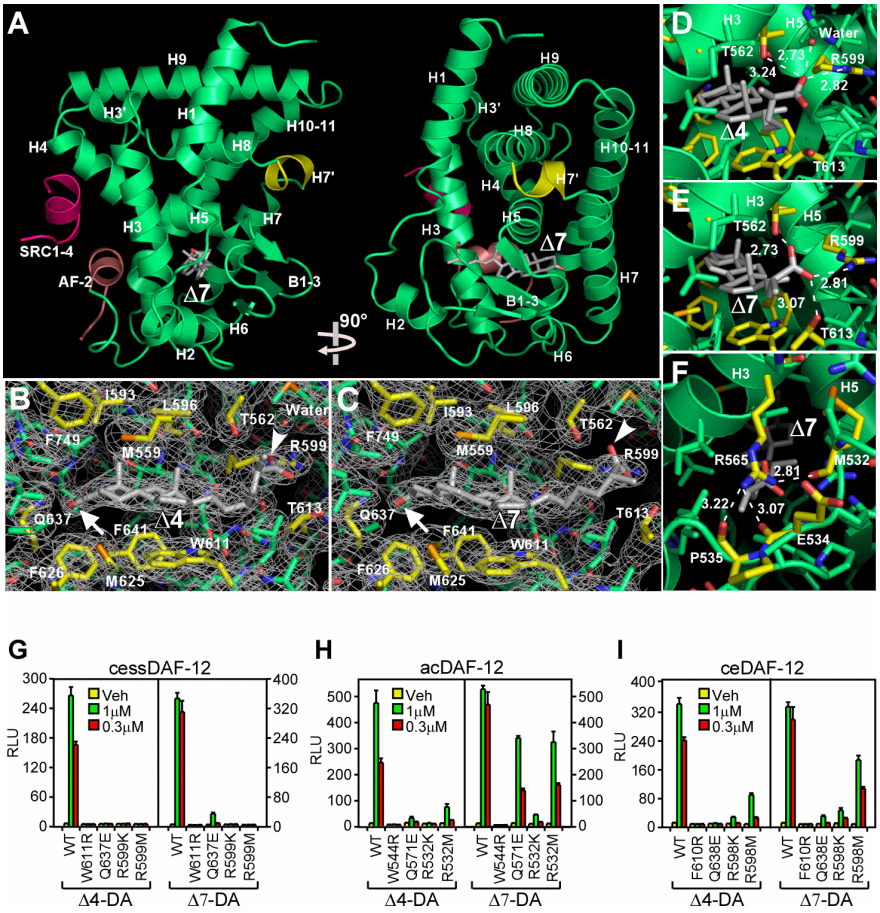

Figure 2-5. X-ray crystal structure of DAF-12 ligand binding domain. (*A*) Ribbon model reveals the overall architecture of the ssDAF-12 ligand binding domain (green) complexed with Δ^7-DA (grey) and the SRC1 coactivator peptide (magenta). The AF-2 helix is shown in salmon. (*B-C*) Electrodensity maps of the ssDAF-12 ligand binding pocket bound to Δ^4-DA (B) or Δ^7-DA (*C*). 3-keto (arrows) and carboxyl (arrowheads) of DA are shown. (*D-E*) H-bonding of ssDAF-12 amino acids directly involved in binding the C_{27}-carboxyl group of Δ^4-DA (*D*) or Δ^7-DA (*E*). (*F*) The "lid" of the ligand binding pocket is formed by H-bond clamping between yellow-colored side chain (R565) and main chain oxygen atoms of M532, E532, and P535. H-bonds are illustrated by white dashed lines with bond lengths noted in Å. (*G-I*), Site-directed mutagenesis reveals differential ligand binding mechanisms for ssDAF-12 (*G*), acDAF-12 (*H*) and ceDAF-12 (*I*). n=3 ± s.d.

2.2.3 DAF-12 Ligand Binding Domain Structure

To provide insight into the biochemistry and pharmacology of DAF-12 ligand binding, we solved the X-ray crystal structure of the ssDAF-12 ligand binding domain complexed with a co-activator LXXLL peptide and both DAs (Figure 2-5*A*). The overall architecture of the ssDAF-12 ligand binding domain is similar to other members of the NR family (Bourguet et al., 1995). It consists of 13 α-helices and three β-sheets, which are packed in a three-layer α-helical sandwich to create a ligand-binding pocket in which DAs are embedded (gray structures). Instead of having a characteristic loop between helices (H) 7 and 8, a unique feature of ssDAF-12 is a short H7' α-helix (yellow in Figure 2-5*A*–*F*). The ssDAF-12 ligand binding domain contains a typical nuclear receptor activation function-2 helix (AF-2) that adopts a characteristic "active" conformation (shown in salmon) as a consequence of its interaction with the co-activator LXXLL peptide (SRC1-4 shown in magenta, Figure 2-5*A*).

As in mammalian nuclear receptors that bind steroid hormones, the ligand-binding pocket of ssDAF-12 is relatively small (517$Å^3$ for Δ^4-DA and 548 $Å^3$ for Δ^7-DA), consistent with the high specificities and affinities of ligand binding. Within the pocket, the lipophilic steroidal rings of DAs are surrounded by non-polar residues (Figure 2-5*B*-*C*), which create a hydrophobic environment critical for the binding of DAs. As evidenced experimentally, introducing a single charged residue (W611R) eliminated receptor activation (Figure 2-5*G*). The two polar groups of DAs are also determinants for ligand recognition: oxygen atoms from the C_3-ketone (arrow) and the C_{27} carboxyl-groups (arrow head) accept hydrogen bonds (H-bonds) donated by polar side chains of various residues in the ligand binding pocket (Figure 2-5*B*-*C*). Disrupting the H-bonds by

either mutating the side chains (Q637E and R599K/M, Figure 3-5*G*) or using DA precursors that lack the C_{27} carboxyl-groups (Figure 2-6) compromised receptor activation. It is noteworthy that the C_{27} carboxyl group of Δ^7-DA forms three H-bonds with ssDAF-12, while the C_{27} carboxyl group of Δ^4-DA only forms two H-bonds (a third H-bond is formed with a water molecule) of weaker strength as indicated by the longer bond lengths with T562 and R599 (Figure 2-5*D, E*). This difference likely explains why Δ^4-DA is a less potent ligand.

Residues outside of the pocket also contribute to ligand binding. Mutation of an arginine conserved in all DAF-12s (R565 in Figure 2-5*F*) disrupted DAF-12 activation by DAs (Figure 2-4*A-E*). Although this residue in ssDAF-12 does not interact with DAs directly, it stabilizes ligand binding by forming H-bonds with the loop region that crosses over the pocket opening (Figure 2-5*F*), thereby functioning as a "lid" to capture the ligand.

Next, we addressed whether the mechanism of ligand binding revealed in the ssDAF-12 structure is conserved in other DAF-12s. In addition to the conserved arginine that is essential for DA activation (Figure 2-3*A-E*), residues involved in ligand recognition are conserved in all DAF-12s (Figure 2-2; Figure 2-5*A-F*). As in ssDAF-12, introducing a single charge into a hydrophobic residue in the core of the pocket (W611R in ssDAF-12, W544R in acDAF-12, F610R in ceDAF-12) abolished receptor activation in all DAF-12s (Figure 2-5*G-I*). However, disruption of residues involved in H-bonding impaired receptor activation in a species-specific manner (compare ssDAF-12 residues Q637E, R599K/M in Figure 2-5*G* to homologous acDAF-12 residues Q571E, R532K/M in Figure 2-5*H* and ceDAF-12 residues Q638E, R598K/M in Figure 2-5*I*). These findings

indicate that DAF-12s bind with DAs through mechanisms that, although similar, also have distinct pharmacological properties.

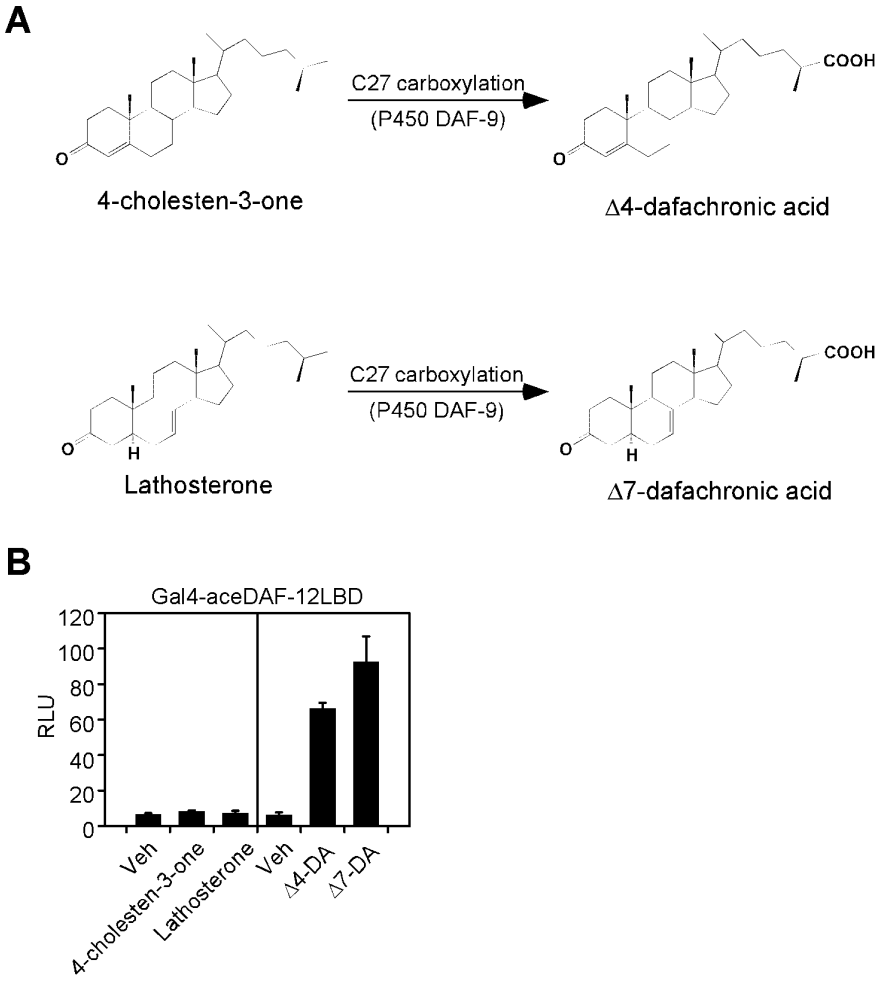

Figure 2-6. The C_{27} carboxyl-group of DAs is important for DAF-12 activation. (*A*) The P450 DAF-9 catalyzes C_{27} oxidation of 4-cholesten-3-one and lathosterone into DAs in *C. elegans*. (*B*) Ligand specific transactivation of hookworm DAF-12 (aceDAF-12) was performed using the Gal4-transactivation assay in HEK293 cells (n = 3 ± s.d.). Ligand concentration = 1 μM.

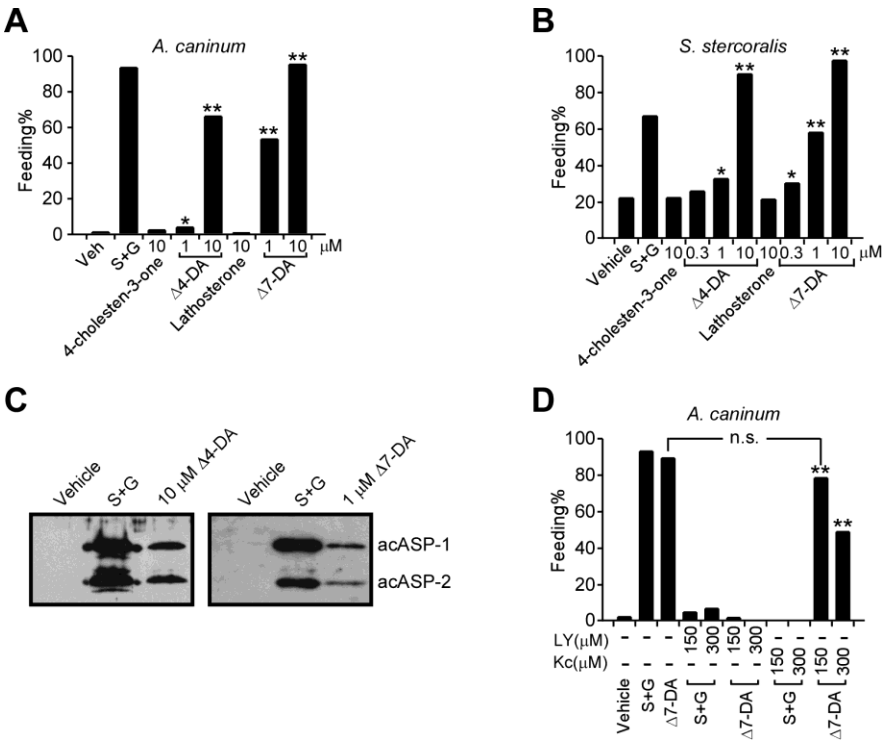

Figure. 2-7. DAF-12 activation induces iL3 recovery. (*A-B*) Dafachronic acids stimulate resumption of feeding in iL3 of *A. caninum*, n=250–1200 (*A*), and *S. stercoralis*, n=725–1081 (*B*). (*C*) Dafachronic acids stimulate ASP secretion by *A. caninum* iL3 larvae. (*D*) Effects of PI3-kinase and P450 inhibitors on Δ^7-DA induced feeding in *A. caninum* iL3 larvae (n=100–407). S+G, 10% canine serum plus 15 mM GSM (A,C,D) or 5 mM GSH (B); LY, PI3-kinase inhibitor LY249002; Kc, P450 inhibitor ketoconazole; *, *P*<0.001; **, *P*<0.0001; n.s., not significant; Chi-square two tailed test, all compared with vehicle treatment unless indicated.

2.2.4 DAF-12 Activation Induces iL3 Recovery

DAs induce dauer recovery in *C. elegans* by activating DAF-12 (Motola et al., 2006). Therefore, we tested whether DAF-12 activation in parasitic nematodes has similar effects. Resumption of feeding is a hallmark of iL3 larvae recovering from the dauer-like stage when they enter their host. This developmental reactivation can be

induced experimentally by providing serum with glutathione (GSH) or S-methyl glutathione (GSM) and works through a mechanism that stimulates the II-S pathway (Brand and Hawdon, 2004; Hawdon and Schad, 1990; Tissenbaum et al., 2000). When tested on the iL3 stage of two hookworm species and *S. stercoralis*, the two DAs induced all of these parasitic larvae to start feeding in a dose dependent manner (Figure 2-7*A,B*; Figure 2-8). In contrast, 4-cholesten-3-one and lathosterone, the metabolic precursors of Δ^4- and Δ^7-DA that do not activate DAF-12, failed to do so. For *Ancylostoma spp.*, a further sign of host-induced iL3 recovery is the secretion of proteins (ASP-1 and ASP-2) that interact with the host's immune system (Hawdon et al., 1996; Hawdon et al., 1999). As shown in Figure 2-7*C*, DAs stimulated the secretion of the pathogenesis-related proteins that are also induced upon treatment with serum and GSH. These results demonstrate that DAF-12 is a key molecular switch that causes resumption of the development in parasitic nematodes.

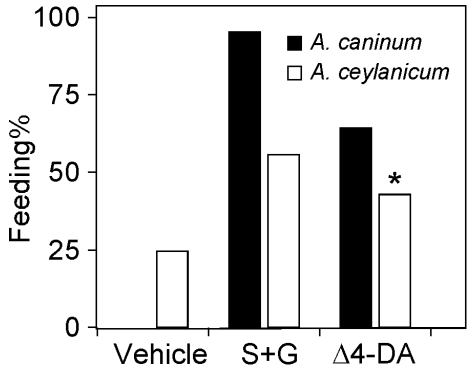

Figure 2-8. Resumption of feeding of in *A. ceylanicum* iL3 larvae is stimulated by DAs. n = 100-58; *, *P*<0.0001; Chi-square two tailed test, all compared with the vehicle treatment.

In *C. elegans*, the cytochrome P450 DAF-9 is required for environmental stimuli to induce dauer recovery. To test whether a similar pathway exists in parasitic nematodes, we used ketoconazole, a broad-spectrum inhibitor for P450s that is known to block steroid hormone synthesis in mammals (Sonino, 1987). Ketoconazole completely abolished iL3 recovery induced by serum/GSM and this inhibition was overcome by pharmacological supplementation with Δ^7-DA (Figure 2-7*D*), suggesting that a P450 is required for parasitic nematode in response to host stimuli. Although to date we have not been able to isolate a DAF-9 homolog from any of the parasitic nematodes, in *A. caninum*, we discovered a partial cDNA encoding a homolog of DAF-36 (Figure 2-9), a Rieske-oxygenase that is upstream of DAF-9 and is also required for generation of the endogenous ligand in *C. elegans*, Δ^7-DA (Rottiers et al., 2006).

Figure 2-9. Sequence alignment of DAF-36 from *C. elegans* and *A. caninum*. acDAF-36 sequence (55380658.eannot.1004) was obtained from the Genome Sequencing Center of Washington University S. Louis (www.nematode.net).

Interestingly, DA did not restore iL3 recovery when the II-S pathway was inhibited using a PI3-kinase inhibitor (LY in Figure 2-7*D*), implying that as in *C. elegans* other outputs from II-S such as FOXO proteins collaborate with DAF-12 to achieve iL3 regulation (Motola et al., 2006). These data support the hypothesis that a conserved steroid hormone/nuclear receptor signaling pathway controls dauer/iL3 recovery in both *C. elegans* and parasitic nematodes (Figure 2-1*A*).

2.2.5 Δ^7-DA Blocks iL3 Larval Development

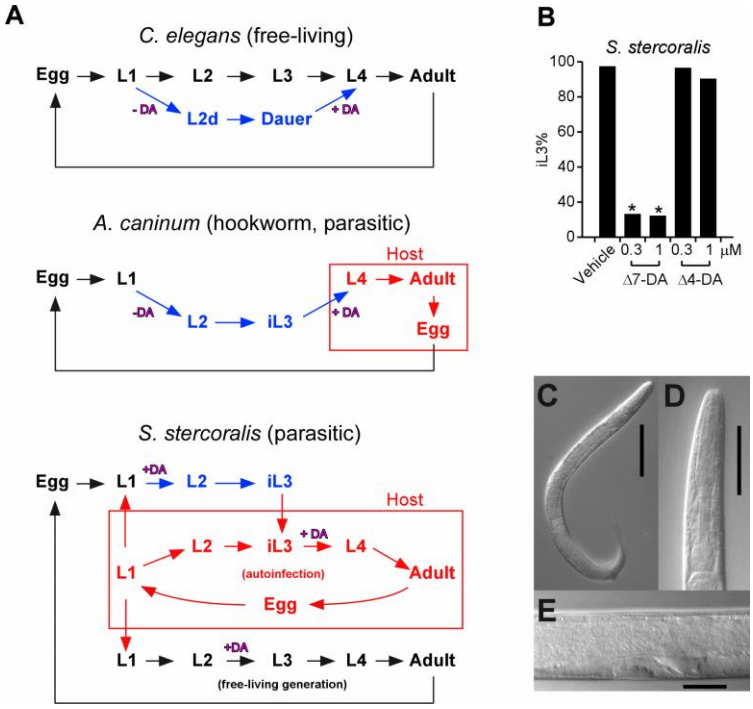

Figure 2-10. Δ7-DA inhibits iL3 development in *S. stercoralis*. (*A*) Comparative life cycles of free-living and parasitic nematode species. (B) Effects of DAs on iL3 formation in S. stercoralis. (C-D) Δ7-DA treatment during early development results in molting-defective, rhabditiform L3/L4 larvae. Whole body, bar=100 μm (*C*); pharynx, bar=50 μm (*D*); vulva, bar=20 μm (*E*). n=113–474; *, *P*<0.0001; Chi-square two tailed test, all compared with vehicle treatment.

In addition to stimulating dauer recovery when bound by ligand, DAF-12 is required for entry into dauer when it is not bound to ligand by acting as a transcriptional repressor of target genes that favor reproductive development (Antebi, 2006; Ludewig et al., 2004b). We tested whether loss of this repression by activating DAF-12 early in development of parasitic nematodes would impair iL3 formation. Unlike hookworm whose progeny directly develop into iL3 larvae in each generation, *S. stercoralis* has an alternative indirect route in which one generation of the free-living life cycle is completed before iL3 progeny are formed (Figure 2-10*A*). This unusual feature of *S. stercoralis* permitted us to obtain synchronized parasite populations for testing. Remarkably, when progeny of the free-living generation of *S. stercoralis* were treated with Δ^7-DA, 88% of the parasites failed to develop into filariform iL3 larvae compared to only 3% when treated with vehicle (Figure 2-10*B*). Importantly, this population of DA-treated larvae developed instead into rhabditiform, molting-defective larvae, which, under continuous exposure to exogenous DA, died within a few days (Figure 2-10*C-E*). The inability of Δ^7-DA to fully rescue the iL3 stage is consistent with its partial agonist activity on ssDAF-12 relative to ceDAF-12 (Figure 2-11). Interestingly, Δ^4-DA had no significant effect on reducing the iL3 population, consistent with the finding that it has even weaker DAF-12 agonist activity (Figure 2-4*E*, Figure 2-11). These findings suggest that Δ^7-DA or a similar congener may have therapeutic utility in the treatment of disseminated strongyloidiasis by preventing iL3 development and therefore terminating the lifecycle of *S. stercoralis*. From an evolutionary standpoint, differential regulation of development by DAF-12 orthologs and their dafachronic acid ligands in free-living nematodes such as *C. elegans*, in strongyloid species with alternate free living cycles, and

in obligate parasites such as hookworms that lack free-living life cycle alternatives, may recapitulate biochemical adaptations that have occurred during the evolution of parasitism in the nematodes.

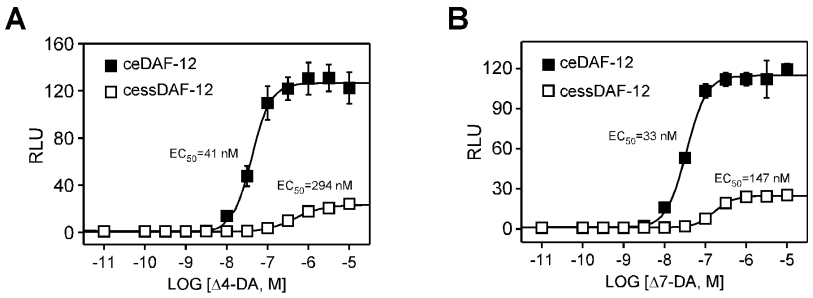

Figure 2-11. DAs differentially activate ceDAF-12 and ssDAF-12. Dose responses of ceDAF-12 and cessDAF-12 to Δ4-DA (*A*) or Δ7-DA (*B*). Co-transfection assays were performed in CV-1 cells (n = 3 ± s.d.).

2.2.6 High Throughput Screening of Parasite DAF-12 for Ligands

Nuclear receptors are considered as one of best drug targets, not only for their key functions in important physiological and pathological processes, but also for the convenient modulation of their activities by small lipophilic molecules (i.e. ligands). As a result, many commercial drugs target nuclear receptors, for therapy of many diseases such as asthma, hypertension, hypocalcemia, thyroid deficiency, dyslipidemia, and diabetes. These facts encouraged us to begin a drug discovery, looking for compounds that targets to the nuclear receptor DAF-12. Given the clinic significance of strongyloidiasis, we selected ssDAF-12 as our initial target.

High throughput screening (HTS) of chemical libraries is a powerful approach for nuclear receptor ligand discovery. To that end, we first modified our regular cell-based reporter assay into a high throughput version and did a pilot test using Δ^7-DA. This pilot

test resulted in a fairly high Z-factor (0.72), which demonstrated that the modified assay was excellent (Z-factor >0.5) for a full-scale, high throughput screening. We then performed a preliminary screen of chemical libraries containing of ~200k small molecules (HTS core, UTSW), and assessed the effect of individual compound, on ssDAF-12 activation. This effort allowed us to identify all ssDAF-12 activators in the chemical libraries.

To confirm the results from the primary screen and test the specificity of the ssDAF-12 activators, we did a cherry-pick screen of a subset of them, in which we not only tested them on ssDAF-12, but also checked their activities on the reporter gene itself and on the mammalian homolog of DAF-12, LXR. The selection of this subset was based on the compound structures, to cover as much diversity of the libraries as possible. It is also based on the compound activities on ssDAF-12 to assure the top activators were included. This selection strategy resulted in 671 preliminary hits for the cherry-picking screening, from which we isolated 54 compounds that activated ssDAF-12 but not the reporter gene (Figure 2-12A). Among them, nine compounds also lacked significant activity on LXR (Figure 2-12B), and these are considered as the specific DAF-12 activators and were thereby selected for further drug development.

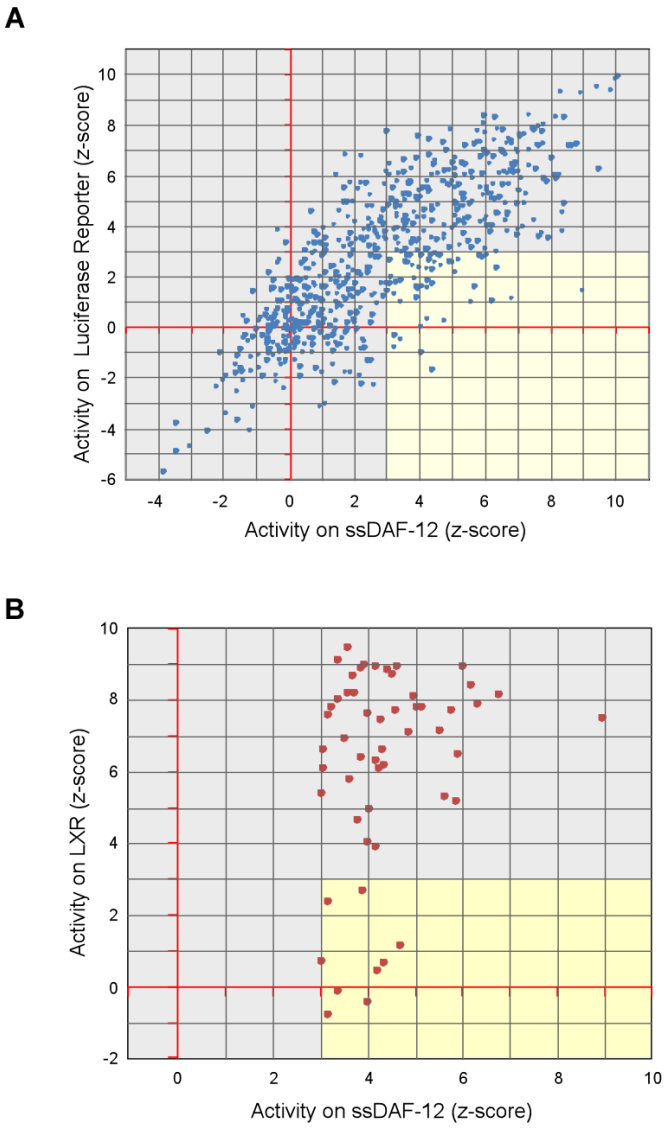

Figure 2-12. High throughput screening of chemical library for ssDAF-12 ligands. Scatter plot of the compound activity (represented as z-score) on ssDAF-12 versus luciferase reporter (A), and ssDAF-12 versus LXR (B). Each dot represents an individual compound which is considered to be active when the Z>3. The yellow rectangles contain the compounds that specifically activate ssDAF-12.

2.3 DISCUSSION

2.3.1 Conserved Hormone Signaling Pathway Controls Dauer/iL3 Diapause in Nematode

In the life cycle of parasitic nematodes, recovery of the dauer-like iL3 larvae after host infection is a poorly understood but essential developmental process. Previous work has shown that successful infection is governed by a variety of host stimuli, including temperature, CO_2 concentration, and serum (Hawdon and Schad, 1990). All of these factors require an insulin-like signaling pathway referred to as II-S (Brand and Hawdon, 2004; Tissenbaum et al., 2000); however, the downstream transducers of this pathway have not been identified (Brand and Hawdon, 2004; Tissenbaum et al., 2000). In the present study we describe the existence of a conserved steroid hormone signaling pathway in parasitic nematodes that is mediated by the nuclear receptor DAF-12 and controls the progression of the parasite's infectious stage, a process that is homologous to *C. elegans* dauer recovery. As part of this study, we identified the *C. elegans* orthologs of DAF-12 in several parasitic nematodes and showed that they bind DA ligands, which in turn stimulate iL3 recovery. Furthermore, we showed DAF-12 activation rescues the serum-induced iL3 recovery that is impaired by P450 inhibition, supporting the notion that within parasitic nematodes, as in *C. elegans*, P450(s) are involved in the production of DAF-12 ligands and are under the regulation of the insulin-like II-S signaling pathway. Moreover, we characterized the 3-dimensional structure of the ssDAF-12 ligand-binding domain and thereby showed the biophysical basis for ligand activation.

From a pharmacological perspective, several aspects of the parasitic DAF-12 pathway are worth highlighting. First, despite the conservation of the pathway with *C.*

elegans and their ability to respond to DAs, parasitic DAF-12 orthologs are not identical among species but share between 42% and 58% similarity in their ligand binding domains. These differences likely explain the higher concentrations required for Δ^4-DA and Δ^7-DA activation of parasite versus *C. elegans* DAF-12. The sequence differences in the various DAF-12 ligand binding domains and their relative affinities for Δ^4-DA and Δ^7-DA suggest that the physiologic ligands for parasite DAF-12s may also vary slightly from species to species. Further support for this notion comes from our inability to identify sequence homologs of the P450 enzyme DAF-9 in the current parasite gene databases or by low-stringency cDNA screening efforts (data not shown). Interestingly, we were able to identify in *A. caninum* a homolog of DAF-36, one of the enzymes required for synthesis of a DAF-9 substrate that is the immediate precursor to Δ^7-DA (Rottiers et al., 2006). This observation raises the intriguing possibility that parasites lack DAF-9 altogether. One interpretation of this finding would be that parasitic nematodes are unable to complete the terminal enzymatic step in DAF-12 ligand synthesis autonomously and instead must rely on a host-specific enzyme for this purpose. Although it remains to be proven, this hypothesis provides an attractive explanation as to why host-specific factors are required for iL3 recovery.

2.3.2 DAF-12 Homologs are Potential Therapeutic Drug Targets for Treating Nematode Parasitic Diseases

A second discovery from this work, which has important pharmacologic implications, is the ability of Δ^7-DA to dramatically reduce the iL3 population in *S. stercoralis*. As observed during dauer recovery in *C. elegans*, DAF-12 activation in both

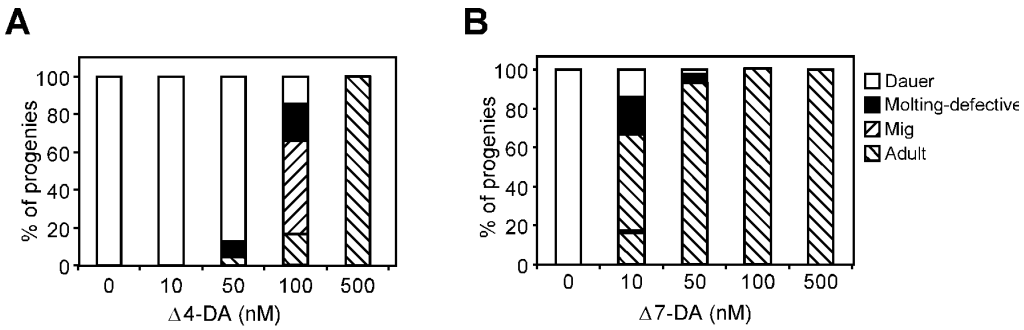

Figure 2-13. Dauer rescue of *daf-9* null mutants by DAs in *C. elegans*. The assay was performed with *daf-9(dh6)* mutants as using Δ^4-DA (*A*) or Δ_7-DA (*B*). Mig, *mig* phenotype.

S. stercoralis and hookworm mediated iL3 recovery. However, as a weak agonist for parasite DAF-12s, Δ^7-DA did not commit the nematode to a complete recovery of its reproductive development, but instead resulted in molting-defective larvae that terminated the parasite's lifecycle. A similar effect of partial DAF-12 activation was also observed during *C. elegans* dauer rescue when using low doses of DAs (Figure 2-13). These findings provide a strong therapeutic rationale for using selective DAF-12 modulators to block iL3 recovery, a strategy that would be strikingly similar to the use of selective estrogen and progesterone modulators in oral contraception.

A clear example of the therapeutic need that would be fulfilled from successfully targeting DAF-12 is disseminated strongyloidiasis. This frequently lethal form of the disease is caused by an autoinfection cycle in which *S. stercoralis* never leaves its host (Figure 2-10*A*), allowing a rapid amplification of the parasite that results from immunosuppression and subsequent multi-organ failure (Viney and Lok, 2007). Thus far, ivermectin is the only drug that has been successful in reducing iL3 hyperinfections, but satisfactory treatments of disseminated strongyloidiasis by this drug have not been established in human being (Fox, 2006). Our study suggests that selective ligand

modulators of DAF-12 might be employed to stop iL3 progression during autoinfection. Taken together, our work provides the first biological, pharmacological, and structural characterization of a nuclear receptor pathway in parasitic species, and thereby serves as the basis for a new therapeutic approach to treating a spectrum of parasitic diseases that collectively affect more than 1 billion people worldwide.

2.3.3 Conserved Energy Metabolic Network in Parasitic Nematodes

In Chapter one, we revealed lipid metabolic enzymes that were controlled by DAF-12. Despite of limited knowledge of the genomes of parasitic nematodes, many of these enzymes could be identified in parasites (Table 2-1). For example, *acs-1*, the enzyme necessary for reproductive growth in *C. elegans*, was found in many species of parasitic nematodes (Figure 2-14). Importantly, it is highly conserved in nematode species but only distantly related to its human homologs (Figure 2-14). Although speculative, these findings provide a strong rationale for treating nematode parasitic diseases with selective inhibitors of the DAF-12-controlled metabolic enzymes. Together with our previous discovery, our work has suggested a spectrum of attractive therapeutic strategies that uniquely aim at iL3 larvae, which infect hosts and are mostly resistant to current anthelmintic drugs.

Table 2-1. Homologs of DAF-12-targeted metabolic genes in parasitic nematodes

C. elegans Gene	Gene Family	Parasitic Nematodes	Accession# (Identity)[a]
acs-3	acyl-CoA synthase	*Ancylostoma caninum*	FC551503.1 (66%)
K08B12.1	Triglyceride lipase	*Brugia malayi*	XM_001892278.1 (51%)
		Strongyloides ratti	FC815643.1 (49%)
		Ancylostoma caninum	CZ205155.1 (62%), CW973657.1 (65%)
F58G1.5	Triglyceride lipase	*Brugia malayi*	XM_001896574.1 (54%)
		Heterodera glycines	CD748763.1 (56%)
		Ancylostoma caninum	CW702349.1 (56%)
cpt-6	CPT-I	*Brugia malayi*	XM_001901719.1 (48%)
		Heterorhabditis bacteriophora	FK802919.1 (67%)
		Haemonchus contortus	CB190924.1 (66%)
		Strongyloides ratti	CZ538717.1 (59%)
		Ancylostoma caninum	GO239192.1 (65%)

a, Homologs are defined by bi-directional blast, which includes a forward blast against parasitic nematode nucleotide databases, and a reverse blast against *C. elegans* nucleotide database.

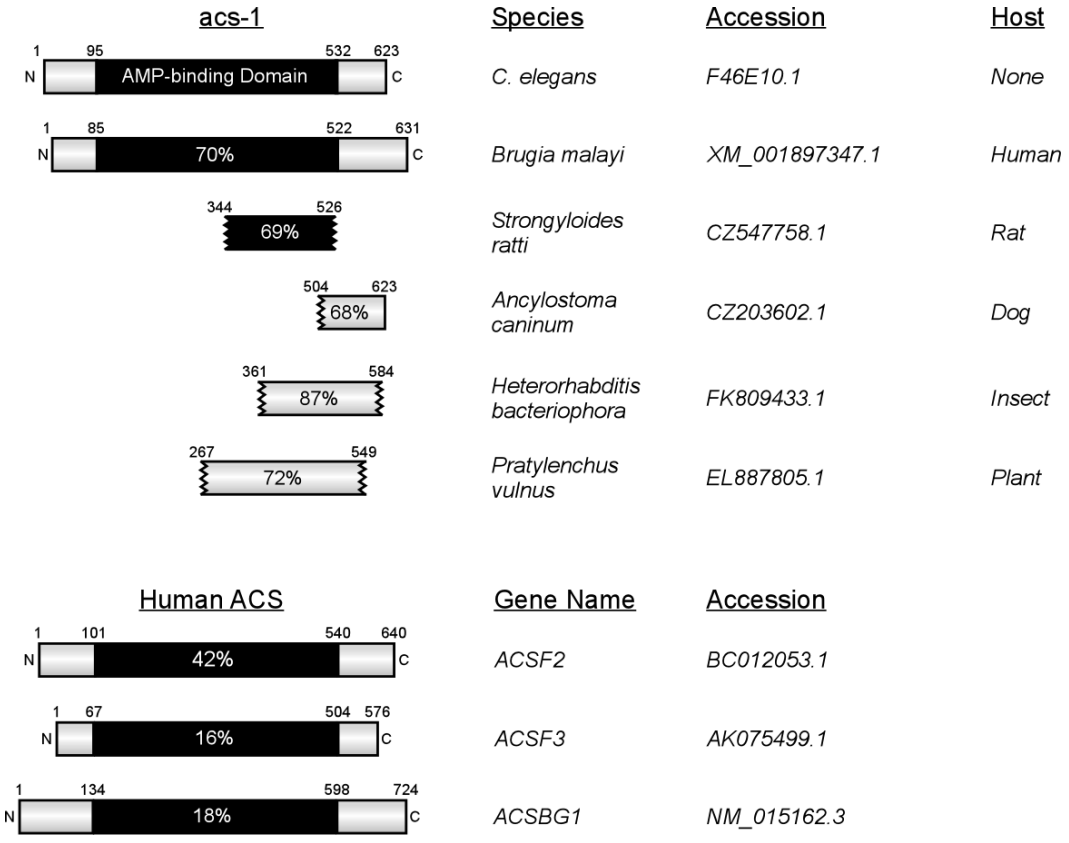

Figure 2-14. *acs-1* homologs in parasitic nematodes and human.

Black boxes indicated the AMP-binding domains, which are defined by pfam. Homologs are determined by bi-directional BLAST. For the incomplete sequences, positions are assigned according to *C. elegans acs-1*.

CHAPTER THREE

DAF-12 in Ruminant and Plant Parasitic Nematodes

3.1 INTRODUCTION

Thus far, the DAF-12 signalling pathway has been characterized in *C. elegans*, hookworm (*Ancylostoma* and *Necator spp.*), *P. pacificus*, and *Strongyloides spp.*, which belong to multiple evolutionary clades of the phylum Nematoda. This observation suggests that DAF-12-mediated diapause regulation might be conserved in other parasitic nematodes. To test this, we selected two other parasitic nematodes, *Haemonchus contortus (H. contortus)* and *Heterodera glycines (H. glycines*), which are two of the most economically important species, and asked whether DAF-12 governs their developmental diapause.

H. contortus is the most pathogenic parasitic nematode for ruminants such as goats and sheep. Adult parasites attach to the abomasal mucosa of the ruminants, where they feed on blood, causing anemia and a series of complications including dehydration, diarrhea, lethargy, reduced growth, loss of reproduction, and eventually death of the infected ruminants. The pathogenic importance of haemonchosis (i.e. the parasitic disease caused by *H. contortus*) is rooted in the parasite's highly prolific life cycle: a fertile female can produce 5,000-10,000 eggs daily, which are expelled with feces, contaminate the whole grazing field and eventually infect other ruminants. In particular, some strains of this parasite have shown multiple drug resistance (MDR) against commonly used anthelmintics and are widely distributed across the world, and therefore are a great threat to the ruminant industries.

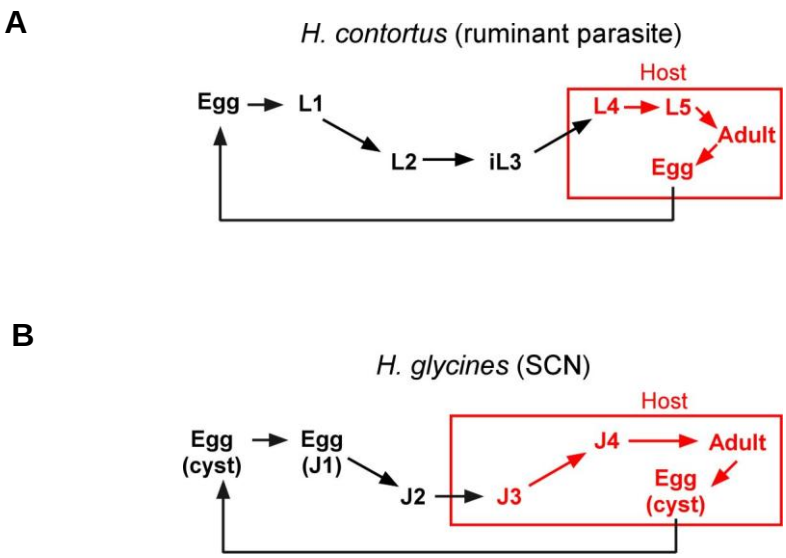

Figure 3-1. Lifecycle of *H. contortus* (A) and *H. glycines* (B). SCN, soybean cyst nematode; iL3, infectious L3.

The lifecycle of *H. contortus* is extremely similar to that of hookworm (Figure 3-1A). The eggs hatch, grow in soil, and arrest as the dauer-like infectious L3 (iL3) larvae. These diapause larvae halt reproductive growth until they enter a host, when they develop into fertile adults and start another round of the lifecycle. Based on this striking similarity, we hypothesized that DAF-12 also controls the regulation of iL3 diapause in *H. contortus*.

H. glycines, also known as soybean cyst nematode (SCN), parasitizes plant hosts including adzuki bean, kidney bean, and soybean. SCN is a major reason for loss of these economically important crops, which costs an estimated 500 million dollars per year in the United States. Crop rotation is the dominant method of combating this parasite: a non-host crop such as corn or wheat is planted for 2-3 years between the planting of susceptible soybean crops. However, this strategy, though effective, is inconvenient,

since any crop rotation plan must be designed based on the knowledge of the existing nematode populations in the field and sometimes is economically unacceptable.

Unlike the parasitic nematodes we addressed previously, *H. glycines* enters developmental diapause mainly as a L1-equivalent larva called the first stage juvenile (J1). The nematode molts once to J1 inside the eggs and upon hatching molts again to J2. This infectious stage of larva then penetrates the root of soybean plants to take in nutrients for reproductive growth to J3, J4, and fertile adults (Figure 4-1B). Each female worm is able to produce up to 600 eggs, but only one third are likely to hatch during the season they are produced. The rest of the eggs are retained within the female body and become dormant cysts after the death of the parent. The additional protection added to these eggs by the cyst wall enables them to survive harsh environments safely in dormancy and hatch when the conditions become favorable for the parasite to reproduce.

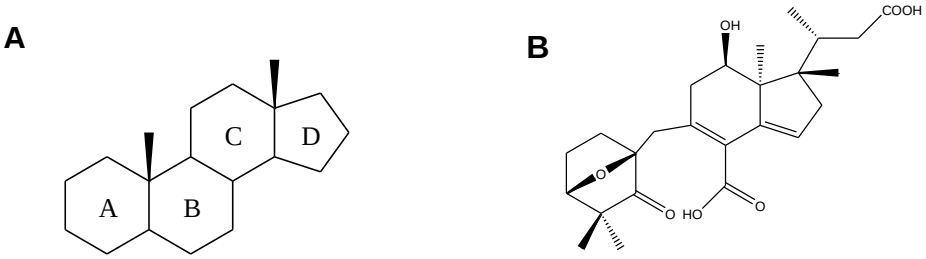

Figure 3-2. Structure of a steroid backbone (A), and glycinoeclepin A (B).

Hatching of the dormant *H. glycines* eggs is stimulated by host signals. The only known host stimulant is glycinoeclepin A (Figure 3-2), a steroid-like compound that was found in root diffuses of soybean plants and effectively induces egg hatching of *H. glycines* at a concentration as low as 2-20 picomolar. However, the molecular mechanism

by which the chemical performs this function remains unknown. Glycinoeclepin A, as illustrated by its chemical structure, seems to be a phytosterol derivative of Δ7-dafachronic acid with its B ring broken in an analogy to 1,25-dihydroxyvitamin D, which is the ligand for the nuclear receptor for Vitamin D (VDR). We therefore hypothesized that glycinoeclepin A might be the ligand of a DAF-12-like nuclear receptor in *H. glycines* (referred to hgDAF-12) that activates the receptor and stimulates egg hatching in the parasite.

3.2 RESULTS AND DISCUSSION

3.2.1 Characterization of DAF-12 in *H. contortus*

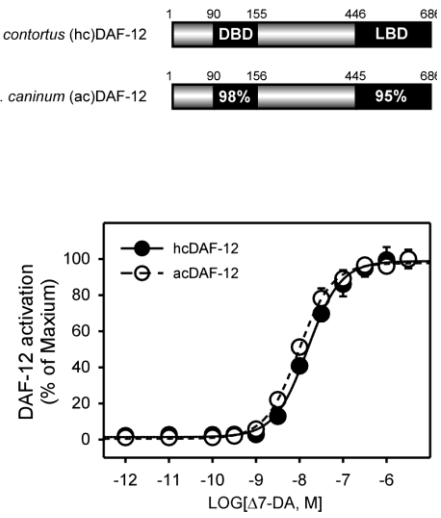

Figure 3-3. Characterization of hcDAF-12. Alignment of hcDAF-12 and acDAF-12 (A), and activation of the DAF-12s by dafachronic acid (B).

By using RACE (Rapid Amplification cDNA Ends), our collaborator has cloned the DAF-12 homolog from the infectious L3 larvae of *H. contortus*. Sequence analysis shows that this nuclear receptor (hcDAF-12) is 98% and 95% identical to hookworm DAF-12 in the DNA-binding domain and ligand-binding domain, respectively (Figure 3-3A). In the same cell-based reporter assay that we used to examine hookworm DAF-12 activation (Figure 2-3D), we found that hcDAF-12 was activated by dafachronic acid as well (Figure 3-3B).

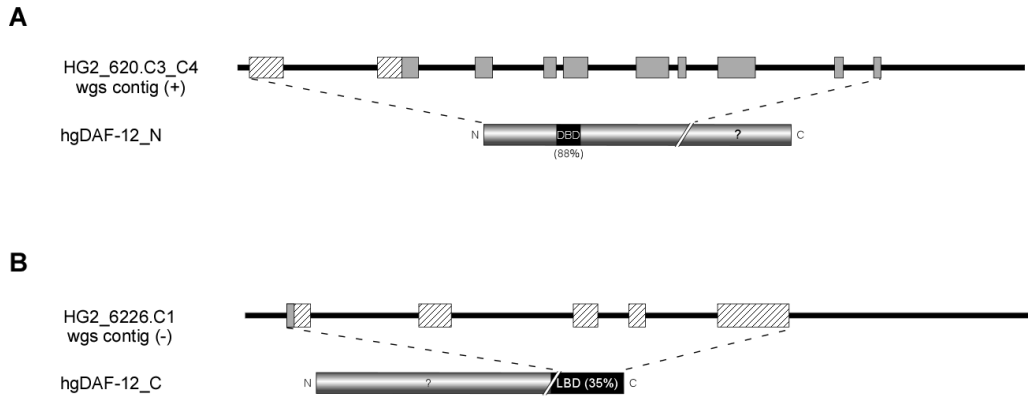

Figure 3-4. DAF-12 homologs in *H. glycines* genome. Schematic illustration of *H. glycines* genomic regions that encode putative hgDAF-12. Boxes indicate exons, which are either predicted by software GeneMark and GeneScan (striped), or revealed by cDNA sequences (grey). +, plus and -, minus strands of the contigs, respectively.

Among all DAF-12 homologs, hcDAF-12 and hookworm DAF-12 share the greatest identity. Their DBDs are 98% identical, and notably, this number remains very high even in the LBD (95%), which is usually less conserved in order to accommodate ligands with various specificities. In line with this, the ligand dafachronic acid activate hc and acDAF-12 with similar potency (EC_{50}~10 nM, Figure 3-3B).

3.2.2 Cloning of DAF-12 in *H. glycines*

Based on our hypothesis, we analyzed the *H. glycines* genome databases for DAF-12 homologs and found several whole genome shotgun (wgs) contigs that appeared to contain pieces of a DAF-12-like gene. HG2_620.C3 and HG2_620.C4 are two overlapping contigs representing a 6.4 kb region of *H. glycines* genome (referred to HG2_620.C3_C4), which contains 10 putative exons that encode the N-terminal 569 aa of hgDAF-12 (referred as hgDAF-12_N, Figure 3-4A). This peptide contains a nuclear receptor DNA binding domain that is 88% identical to that of *C. elegans* DAF-12. The

HG2_6226 contig contains 3.9 kb of genomic DNA with 5 putative exons and encodes part of the ligand binding domain of hgDAF-12 (referred to hgDAF-12_C, Figure 3-4B). Further analysis showed that DAF-12 is the most similar to both hgDAF-12_N and _C in the whole *C. elegans* genome, as revealed by reverse BLAST search. This finding indicates that the gene we identified encodes a piece of the *H. glycines* DAF-12 homolog.

In order to clone this nuclear receptor, we first constructed a cDNA library containing the whole mRNA transcriptome from *H. glycines* eggs, which includes ~5 million independent clones bearing *H. glycines* cDNA inserts averaging 1.1 kb in length (data not shown). We then tested for the presence of the putative hgDAF-12 in our library. We detected the presence of both hgDAF-12_N and _C in the library, as evidenced by specific PCR amplifications (Figure 3-5). Following a similar PCR strategy, we cloned a 1230-bp fragment from hgDAF-12_N, including the DNA binding domain (Figure 3-4A, grey exons).

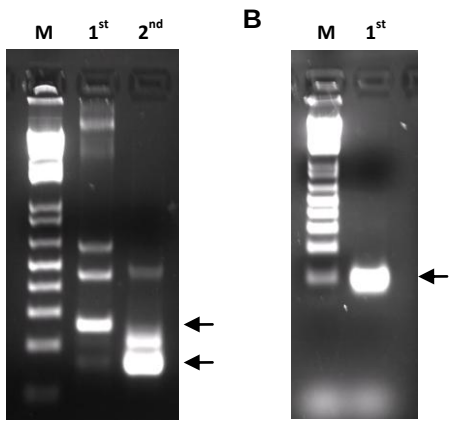

Figure 3-5. Detection of hgDAF-12_N (A) and hgDAF-12_C (B) in cDNA library. M, DNA marker; 1st, the first round of PCR; 2nd, the second round PCR with nested primers; arrows, amplification products from hgDAF-12, which are identified by DNA sequencing.

In contrast to hcDAF-12, hgDAF-12 is much less similar to other DAF-12s. Its DBD and LBD are just 88% and 35% identical to *C. elegans* DAF-12, respectively. For comparison, acDAF-12, hcDAF-12 and ssDAF-12 show 95%, 96% and 95% identity in the DBD, and 58%, 57%, and 42% identity, respectively, in the LBD. Despite the lower homology in general, hgDAF-12

preserves the structural determinants that specify the functionality of DAF-12s. For example, the P-box in the DBD that provides a nuclear receptor with DNA binding specificity is the same in hgDAF-12 as in the other DAF-12s. Similarly, the LBD residues that are directly involved in DAF-12/ligand interaction are highly conserved as well. These facts also suggest that hgDAF-12 might act as a canonical DAF-12 in the parasite *H. glycines*.

In summary, this study identified DAF-12 homologs in *H. contortus* and *H. glycines*. In the future, we will test whether hcDAF-12 can bind dafachronic acids in an in vitro alpha-screening assay, and whether its function is conserved with respect to L3 diapause regulation. In order to clone the full-length of hgDAF-12, we are currently employing various methods such as colony hybridization and RACE. Once the cloning is complete, we will test whether dafachronic acids can activate hgDAF-12. We will also test its response to glycinoeclepin A, which we are attempting to obtain by either chemical synthesis or purification from soybean plants. These efforts will enable us to better understand how the nematode diapause is regulated, which will reveal novel drug targets and efficient therapeutic strategies to control parasitic nematodes that cause great economical losses.

CHAPTER FOUR

Materials and Methods

4.1 Reagents and Nematode Strains

Δ^7-dafachronic was obtained from Dr. E. J. Corey (Harvard University) or made as described (Sharma et al., 2009). 4-cholesten-3-one, etomoxir and 2-deoxy-D-glucose (2-DG) were purchased from Sigma. The *C. elegans* strains *din-1(dh127)*, *din-1daf-9(dh127;dh6)*, and *din-1daf-12(dh127;rh61rh411)* were generous gifts from Dr. Adam Antebi (Baylor College Medicine). The *daf-9(dh6)* strain was isolated by picking GFP negative progeny of *daf-9 (dh6, dhEx24)* (Dr. Adam Antebi) and was maintained in presence of dafachronic acid. The *daf-2(e1368)* and *daf-7(e1372)* strains were from *C. elegans* Genome Center (Univ. of Minnesota). Nematode strains were maintained on NGM-agar with OP50 bacteria lawn at 16 ℃ (*daf-7*), 20 ℃ (*daf-2*), or room temperature (all other strains).

4.2 cDNA and Plasmids

acDAF-12 and naDAF-12 cDNAs were isolated from iL3 libraries of *A. caninum* and *N. americanus*; aceDAF-12LBD cDNA (database accession number, pk90d07) was obtained from the Genome Sequencing Center, Washington University and ssDAF-12 was a gift from Dr. Afzal Siddiqui (NCBI accession number, AF145048) (Siddiqui et al., 2000). cDNAs were amplified by PCR and inserted into the indicated expression vectors, and verified by sequencing.

4.3 Triglyceride Content Assay and ATP Measurement

Vehicle control or dafachronic acid solutions were mixed with 5×concentrated OP50 bacteria from an overnight culture and were loaded on NGM-agar plates. Synchronized L1 larvae, which were achieved by overnight egg hatching, were cultured on these plates at 25℃ for 22.5 hrs. The resulting L3 worms were then collected, washed, and resuspended in M9 buffer. After lysing the worms by sonication, total protein was quantified by Bradford assay (Bio-Rad). Lysates were then centrifuged at 4℃, 13,000×g, and supernatants were saved for further measurement. For total triglycerides (i.e. triglycerides and free glycerol), triolein standards (Sigma) or the supernatants were mixed with Infinity Triglyceride Reagent (Thermo Sci), and absorbance at 520 nm was measured following an incubation at room temperature for 20 min. Free glycerol in the same samples was also measured, by using Free Glycerol Reagent (Sigma) according to the manufacturer's instructions. Triglyceride contents were calculated by subtracting free glycerol from total triglycerides, followed by normalization to the amounts of protein.

Steady state ATP levels were measured by Cell-Tiler Glo Luminescence Kit (Promega). Worm lysates prepared as in TG assay and ATP standards (Roche) were mixed with Cell-Tiler Glo reagent at 1:1 ratio. After 10 min incubation at room temperature, luminescence was read using a Victor Plate Reader (Perkin Elmer). The amount of ATP in samples was then calculated from a standard curve and normalized to the protein amounts.

4.4 Oxygen Consumption

Worms treated and collected as described in triglyceride assay were split into two aliquots. OP50 suspension was mixed with one of the aliquots or an equal volume of M9 buffer, and transferred to Oxygen Biosensor plate (BD Bioscience), which fluoresces

with intensity inversely proportional to the aqueous oxygen concentration. The plate was then sealed by optical cover and kept at room temperature for the indicated periods. Fluorescence was then detected by a Victor Plate Reader (Perkin Elmer) at excitation/emission of 585/630 nm. The other aliquot of worms was sonicated and used for protein quantification. Oxygen consumption was presented as normalized arbitrary fluorescent units (AFU) by subtracting fluorescence signal of M9 control from that of the worm aliquot, and dividing by protein amount.

4.5 Dietary Fatty Acid Uptake

Synchronized L1 worms were cultured on NGM-agar plates and treated same as in oxygen consumption assay. After 22.5 hrs incubation at 25℃, L3 worms were collected and suspended in M9 buffer containing OP50 and 250 nM of fluoresent tracer (C1-BODIPY-C12 fatty acid, Invitrogen). Following 1 hr uptake at 25℃, the worms were washed and mounted, and photos were taken under fluoresence microscopy. Fluoresence density of each worm was quantified by the software Image-J. AFU, arbitrary fluoresence units. Each dot represents total fluoresence units from a single worm. Data were collected from two independent experiments.

4.6 Quantitative Real Time PCR (qPCR)

qPCR and data analysis was performed as described (Bookout et al., 2006), with a few modifications. For RNA extraction, nematode pellets were mixed with 10 volumes of RNA-STAT60 (AMS Biotechnology) and subject to freeze-thaw cycles to release the worm contents. Chloroform was then mixed with the lysates, and phase separation was performed by centrifugation at 10,000×g for 15 min at 4℃. The aqueous phase was then transferred to a fresh tube, wherein RNA was precipitated by addition of isopropanol,

followed by 4℃ centrifugation at 13,000×g for 20 min. The resulting RNA pellets were washed with 75% ethanol, air dried, and dissolved in nuclease-free water (Invitrogen). The RNAs were then treated with DNAse-I (Roche) and used for cDNA synthesis. The mRNA expression of the indicated genes was detected by SYBR green-based real-time PCR assay (Applied Biosystem Inc), and data were analyzed by the ΔΔCt method.

4.7 Electrophoretic Mobility Shift Assay

Sequences of double-stranded oligonucleotides as shown in Table 1-2 were synthesized with "agct"-overhang at 5 prime. DAF-12 protein was made by TNT Quick-Coupled Transcription/Translation System (Promega) following the manufacturers' instructions. With same procedure, control TNT lysates were also made by replacing the DAF-12 expression plasmid with empty vector. For pre-binding, 2 μl DAF-12 protein or control TNT lysate was incubated on ice for 30 min with poly-[dI-dC] (Sigma) and non-specific single-stranded oligonucleotides in 20 μl of reaction consisting of 20 mM HEPES (PH 7.4), 75 mM KCl, 7.5% glycerol, 0.1% IGEPAL CA-630 (Sigma), and 2 mM DTT. ^{32}P-labeled oligonucleotide probes (labeled by end-filling) were then added into the pre-binding reactions for 30 min at room temperature, allowing DAF-12 binding to DNA probes. The mixtures were analyzed by 5% polyacrylamide gel, and the binding was visualized by vacuum-drying the gels and exposing to X-ray films. For competitive binding experiments, 20 or 200 times excess unlabeled double-stranded oligonucleotides were also included in the binding reaction.

4.8 Cell-based Reporter Assays

HEK293 and CV-1 cells were cultured and transfected in 96-well plates as described (Motola et al., 2006; Sharma et al., 2009; Wang et al., 2009) using 50 ng

luciferase reporter, 10 ng CMX-β-galactosidase reporter, and 15 ng nuclear receptor expression plasmids. Ethanol or the indicated compounds were then added to each well 8 hrs post-transfection. Following a 16 hr incubation, the cells were harvested and analyzed for luciferase and β-galactosidase activities. The luciferase reporter plasmids are constructed by insertion of Gal4 or putative DAF-12 response elements before the proximal HSV-tk minimal promoter. Relative luciferase activity (RLU) was defined as the activity of luciferase normalized to that of β-galactosidase. Fold induction is ratio of the RLU in DA to vehicle treated cells. Data represent the mean ± s.d. from triplicate assays and were plotted using Sigma Plot software.

4.9 RNAi, Inhibitor Treatment and Rescue Assays

Gene-specific silencing was achieved by the feeding RNAi method (Kamath and Ahringer, 2003), with a few modifications. Culture of HT115 bacteria transformed with RNAi plasmids was loaded on NGM-agar containing 1 mM IPTG and 50 mg/ml ampicillin. Double-stranded RNAs were induced by keeping the plates at room temperature overnight. In the following morning, the plates were loaded with PBS buffer containing vehicle control or 200 nM Δ^7-dafachronic acid. Synchronized L1 worms were transferred, and the plates were incubated at 25 ℃. The developomental phenotypes were observed 60 hrs later. In the inhibitor experiments, etomoxir or 2-deoxy-D-glucose was added when NGM-agar plates were pooled, and 5× concentrated OP50 culture was used as the food source instead of HT115.

4.10 *C. elegans* Reproductive Growth

Reproductive growth of *C. elegans* was measured either by L4-young adult transition assay or by egg laying assay. For the L4-YA transition assay, synchronized L1s were cultured on NGM-agar plates pre-loaded with 5× concentrated HT115 culture containing vehicle control or 200 nM Δ^7-dafachronic acid. The worms were grown at 20 ℃ and young adults were counted and then removed at each indicated time point. Data are presented as the percentage of young adults in the whole population. Worms for egg laying assay were processed similarly except OP50 bacteria was used as the food source and the worms were grown at 25 ℃. At the indicated time points, 10-15 worms were transferred to fresh plates pre-loaded with a bacteria lawn. After 2.5 hrs of incubation at 25 ℃, the worms were removed, and the eggs left on the plates were then counted. Data were presented as the number of eggs laid per worm per hour.

4.11 Parasite Studies

Free-living adult males and females or infective third-stage larvae (iL3s) were obtained from charcoal coprocultures of the feces of dogs experimentally infected with *S. stercoralis* or *A. caninum*, isolated by the Baermann funnel technique, and decontaminated as described (Ashton et al., 2007; Hawdon and Schad, 1990; Lok, 2007). For iL3 formation studies, synchronous cohorts of eggs were obtained by allowing 40-50 females to oviposit in the presence of males for 3 hrs on plates that had been treated with ethanol vehicle or DA as described previously (Motola et al., 2006; Sharma et al., 2008). Adult worms were removed from plates following oviposition and cultures were sealed with parafilm and incubated at 20°C for 72 hrs. Rate of iL3 formation was the percentage of iL3 in total viable progenies. Data were gathered from triplicate assays. For feeding studies, iL3 larvae were cultured in DMEM (*S. stercoralis*) or RPMI-c (*A. caninum*) with

antibiotics and treated with ethanol or the indicated agents. All parasites were cultured in an atmosphere of 5% CO_2 in air under the specified conditions at 22°C for 21 hrs (*S. stercoralis*) or at 37°C for 24 hrs (*A. caninum*). After this interval, FITC-BSA (Invitrogen) was added for 2 hrs and then resumption of pharyngeal pumping was assayed by monitoring ingestion of the fluorescent tracker by using fluorescence microscopy. The positive controls (S+G) were worms treated by 10% caninum serum with glutathione (*S. stercoralis*) or S-methyl glutathione (*A. caninum*) at 37°C. Feeding rate was the percentage of iL3s with green guts in the whole population. Data were gathered from at least duplicate assays.

4.12 *Ancylostoma*-Secreted Protein (ASP) Secretion Assay

The assay was performed as described (Hawdon et al., 1996; Hawdon et al., 1999). Briefly, ~5,000 *A. caninum* iL3 were cultured and treated as above for 24 hrs. The supernatant was filtered through a 0.2 mm HT Tuffryn syringe filter (Pall Corporation, Ann Arbor, MI) and concentrated by ultrafiltration. The resulting concentrated supernatants were then subjected to standard Western Blot assay. ASPs in the supernatants were detected by anti-ASP rabbit serum and visualized by ECL (Amersham Pharmacia Biotech).

4.13 Ligand Binding Assay

Parasite DAF-12 ligand binding domains were expressed in BL21 (DE3) cells as 6X His-GST fusion proteins. Ligand binding was determined by Alpha screening assay kit (Perkin-Elmer). The experiments were conducted with approximately 40 nM receptor ligand binding domain and 10 nM biotinylated SRC1–4 peptide (QKPTSGPQAQQKSLLQQLLTE) in the presence of 20 μg/ml donor and acceptor

beads in a buffer containing 50 mM MOPS, 50 mM NaF, 50 mM CHAPS, and 0.1 mg/ml bovine serum albumin, all adjusted to a pH of 7.4.

4.14 DAF-12 Protein Purification

ssDAF-12LBD (residues 510–753) was expressed as a 6x Histidine-SUMO fusion protein from the expression vector pSUMO (LifeSensors). BL21 (DE3) cells were grown to an OD600 of approximately 1.0, induced with 50 μM of isopropyl-β-D-thiogalactopyranoside (IPTG) at 16 ℃, and harvested in extract buffer (10 mM Tris pH7.3/200 mM NaCl/10% glycerol/0.25mg/ml lysozyme/100 μM PMSF). Cells were passed through a French Press with the pressure set at 1kPa. The resulting lysate was centrifuged at 20,000 rpm for 30 min, and the supernatant was added over a pre-equilibrated 25 ml Ni NTA fast flow column (Amersham Biosciences), which was washed with 600 ml of buffer A (20 mM Tris pH 8.0, 200 mM NaCl, 50 mM imidazole and 10% glycerol). The 6x Histidine-SUMO was eluted using buffer A supplemented with 250 mM imidazole, cleaved overnight with 1/2000 SUMO protease at 4 ℃ and then dialyzed against 4 litters of 20 mM Tris pH 8.0, 200 mM NaCl and 10% glycerol. The protein was then loaded onto a pre-equilibrated 10 ml Ni NTA chelating sepharose column (Amersham Biosciences) and eluted at 10% buffer B (10 mM Tris pH 8.0/1 M NaCl/10% glycerol/500 mM imidazole). EDTA and DTT were then added to 1 mM and ssDAF-12LBD was concentrated and further purification by a gel filtration column in the buffer of 20 mM Tris pH 8.0, 200 mM NaCl, and 10% glycerol (10 mg/ml for crystallization). A typical yield of the purified ssDAF12 was about 3 mg/L of cells.

4.15 Crystallization, Data Collection and Structure Determination

Crystals of ssDAF12 ligand binding domain were grown at 20℃ in hanging drops containing 1 μl of the above protein solution and 1 μl of well solution containing 0.2M $(NH_4)_2SO_4$, 28% PEG 8000, and 10% 3MPT 135 for the protein complex ssDAF12/Δ^4-DA or 0.2M $(NH_4)_2SO_4$, 32% PEG 6000 and 5% mPEG350 for ssDAF12/Δ^7-DA. Crystals were flash frozen in liquid nitrogen before data collection. The datasets were collected with a MAR300 CCD detector at the ID line of sector-23 at the Advanced Photon Source at Argonne National Laboratory (Argonne, Illinois, United States). The observed reflections were reduced, merged, and scaled with DENZO and SCALEPACK in the HKL2000 package. Molecular replacement was performed by using CCP4 program "Phaser". Program "O" and Quanta (Accelrys) were used to manually fit the protein model. Model refinement was performed with CNS and REFMAC. The volumes of the ligand binding pocket were calculated with the program Voidoo using program default parameters and a probe with a radius of 1.4Å. All figures were prepared using PyMOL.

BIBLIOGRAPHY

Angelo, G., and Van Gilst, M.R. (2009). Starvation protects germline stem cells and extends reproductive longevity in *C. elegans*. Science *326*, 954-958.

Antebi, A. (2006). Nuclear hormone receptors in *C. elegans*. WormBook, 1-13.

Ashton, F.T., Zhu, X., Boston, R., Lok, J.B., and Schad, G.A. (2007). *Strongyloides stercoralis*: Amphidial neuron pair ASJ triggers significant resumption of development by infective larvae under host-mimicking in vitro conditions. Exp Parasitol *115*, 92-97.

Bethke, A., Fielenbach, N., Wang, Z., Mangelsdorf, D.J., and Antebi, A. (2009). Nuclear hormone receptor regulation of microRNAs controls developmental progression. Science *324*, 95-98.

Bookout, A.L., Cummins, C.L., Mangelsdorf, D.J., Pesola, J.M., and Kramer, M.F. (2006). High-throughput real-time quantitative reverse transcription PCR. Curr Protoc Mol Biol *Chapter 15*, Unit 15 18.

Bourguet, W., Ruff, M., Chambon, P., Gronemeyer, H., and Moras, D. (1995). Crystal structure of the ligand-binding domain of the human nuclear receptor RXR-alpha. Nature *375*, 377-382.

Braeckman, B.P., Houthoofd, K., and Vanfleteren, J.R. (2009). Intermediary metabolism. WormBook, 1-24.

Brand, A., and Hawdon, J.M. (2004). Phosphoinositide-3-OH-kinase inhibitor LY294002 prevents activation of *Ancylostoma caninum* and *Ancylostoma ceylanicum* third-stage infective larvae. Int J Parasitol *34*, 909-914.

Fox, L.M. (2006). Ivermectin: uses and impact 20 years on. Curr Opin Infect Dis *19*, 588-593.

Gerisch, B., Weitzel, C., Kober-Eisermann, C., Rottiers, V., and Antebi, A. (2001). A hormonal signaling pathway influencing *C. elegans* metabolism, reproductive development, and life span. Dev Cell *1*, 841-851.

Hammell, C.M., Karp, X., and Ambros, V. (2009). A feedback circuit involving let-7-family miRNAs and DAF-12 integrates environmental signals and developmental timing in *Caenorhabditis elegans*. Proc Natl Acad Sci U S A *106*, 18668-18673.

Hannich, J.T., Entchev, E.V., Mende, F., Boytchev, H., Martin, R., Zagoriy, V., Theumer, G., Riezman, I., Riezman, H., Knolker, H.J., *et al.* (2009). Methylation of the sterol nucleus by STRM-1 regulates dauer larva formation in *Caenorhabditis elegans*. Dev Cell *16*, 833-843.

Hawdon, J.M., Jones, B.F., Hoffman, D.R., and Hotez, P.J. (1996). Cloning and characterization of Ancylostoma-secreted protein. A novel protein associated with the transition to parasitism by infective hookworm larvae. J Biol Chem *271*, 6672-6678.

Hawdon, J.M., Narasimhan, S., and Hotez, P.J. (1999). Ancylostoma secreted protein 2: cloning and characterization of a second member of a family of nematode secreted proteins from Ancylostoma caninum. Mol Biochem Parasitol *99*, 149-165.

Hawdon, J.M., and Schad, G.A. (1990). Serum-stimulated feeding in vitro by third-stage infective larvae of the canine hookworm *Ancylostoma caninum*. J Parasitol *76*, 394-398.

Henderson, S.T., and Johnson, T.E. (2001). daf-16 integrates developmental and environmental inputs to mediate aging in the nematode *Caenorhabditis elegans*. Curr Biol *11*, 1975-1980.

Horner, M.A., Pardee, K., Liu, S., King-Jones, K., Lajoie, G., Edwards, A., Krause, H.M., and Thummel, C.S. (2009). The *Drosophila* DHR96 nuclear receptor binds cholesterol and regulates cholesterol homeostasis. Genes Dev *23*, 2711-2716.

Hotez, P., Hawdon, J., and Schad, G.A. (1993). Hookworm larval infectivity, arrest and amphiparatenesis: the *Caenorhabditis elegans* daf-c paradigm. Parasitology Today *9*, 23-26.

Hotez, P.J., Bethony, J., Bottazzi, M.E., Brooker, S., Diemert, D., and Loukas, A. (2006). New technologies for the control of human hookworm infection. Trends Parasitol *22*, 327-331.

Igra-Siegman, Y., Kapila, R., Sen, P., Kaminski, Z.C., and Louria, D.B. (1981). Syndrome of hyperinfection with *Strongyloides stercoralis*. Rev Infect Dis *3*, 397-407.

Jasmer, D.P., Goverse, A., and Smant, G. (2003). Parasitic nematode interactions with mammals and plants. Annu Rev Phytopathol *41*, 245-270.

Kalaany, N.Y., and Mangelsdorf, D.J. (2006). LXRS and FXR: the yin and yang of cholesterol and fat metabolism. Annu Rev Physiol *68*, 159-191.

Kamath, R.S., and Ahringer, J. (2003). Genome-wide RNAi screening in *Caenorhabditis elegans*. Methods *30*, 313-321.

Kaplan, R.M. (2004). Drug resistance in nematodes of veterinary importance: a status report. Trends Parasitol *20*, 477-481.

Lok, J.B. (2007). *Strongyloides stercoralis*: a model for translational research on parasitic nematode biology. WormBook, 1-18.

Ludewig, A.H., Kober-Eisermann, C., Weitzel, C., Bethke, A., Neubert, K., Gerisch, B., Hutter, H., and Antebi, A. (2004a). A novel nuclear receptor/coregulator complex controls *C. elegans* lipid metabolism, larval development, and aging. Genes Dev *18*, 2120-2133.

Ludewig, A.H., Kober-Eisermann, C., Weitzel, C., Bethke, A., Neubert, K., Gerisch, B., Hutter, H., and Antebi, A. (2004b). A novel nuclear receptor/coregulator complex controls *C. elegans* lipid metabolism, larval development, and aging. Genes Dev *18*, 2120-2133.

Mooijaart, S.P., Brandt, B.W., Baldal, E.A., Pijpe, J., Kuningas, M., Beekman, M., Zwaan, B.J., Slagboom, P.E., Westendorp, R.G., and van Heemst, D. (2005). *C. elegans* DAF-12, Nuclear Hormone Receptors and human longevity and disease at old age. Ageing Res Rev *4*, 351-371.

Motola, D.L., Cummins, C.L., Rottiers, V., Sharma, K.K., Li, T., Li, Y., Suino-Powell, K., Xu, H.E., Auchus, R.J., Antebi, A., *et al.* (2006). Identification of ligands for DAF-12 that govern dauer formation and reproduction in *C. elegans*. Cell *124*, 1209-1223.

Muller, R. (2002). The Nematodes. In Worms and Human Disease, R. Muller, ed. (New York, CABI), pp. 115-138.

Murphy, C.T., McCarroll, S.A., Bargmann, C.I., Fraser, A., Kamath, R.S., Ahringer, J., Li, H., and Kenyon, C. (2003). Genes that act downstream of DAF-16 to influence the lifespan of *Caenorhabditis elegans*. Nature *424*, 277-283.

Riddle, D.L., and Albert, P.S. (1997). Genetic and Environmental Regulation of Dauer Larva Development. In C ELEGANS II, D.L. Riddle, T. Blumenthal, B.J. Meyer, and J.R. Priess, eds. (New York, Cold Spring Harbor Laboratory Press), pp. 739-768.

Rottiers, V., Motola, D.L., Gerisch, B., Cummins, C.L., Nishiwaki, K., Mangelsdorf, D.J., and Antebi, A. (2006). Hormonal control of *C. elegans* dauer formation and life span by a Rieske-like oxygenase. Dev Cell *10*, 473-482.

Sharma, K.K., Wang, Z., Motola, D.L., Cummins, C.L., Mangelsdorf, D.J., and Auchus, R.J. (2009). Synthesis and activity of dafachronic acid ligands for the *C. elegans* DAF-12 nuclear hormone receptor. Mol Endocrinol *23*, 640-648.

Shostak, Y., Van Gilst, M.R., Antebi, A., and Yamamoto, K.R. (2004). Identification of *C. elegans* DAF-12-binding sites, response elements, and target genes. Genes Dev *18*, 2529-2544.

Siddiqui, A.A., Stanley, C.S., Skelly, P.J., and Berk, S.L. (2000). A cDNA encoding a nuclear hormone receptor of the steroid/thyroid hormone-receptor superfamily from the human parasitic nematode *Strongyloides stercoralis*. Parasitol Res *86*, 24-29.

Sieber, M.H., and Thummel, C.S. (2009). The DHR96 nuclear receptor controls triacylglycerol homeostasis in *Drosophila*. Cell Metab *10*, 481-490.

Sonino, N. (1987). The use of ketoconazole as an inhibitor of steroid production. N Engl J Med *317*, 812-818.

Tissenbaum, H.A., Hawdon, J., Perregaux, M., Hotez, P., Guarente, L., and Ruvkun, G. (2000). A common muscarinic pathway for diapause recovery in the distantly related nematode species *Caenorhabditis elegans* and *Ancylostoma caninum*. Proc Natl Acad Sci U S A *97*, 460-465.

Van Gilst, M.R., Hadjivassiliou, H., Jolly, A., and Yamamoto, K.R. (2005a). Nuclear hormone receptor NHR-49 controls fat consumption and fatty acid composition in *C. elegans*. PLoS Biol *3*, e53.

Van Gilst, M.R., Hadjivassiliou, H., and Yamamoto, K.R. (2005b). A *Caenorhabditis elegans* nutrient response system partially dependent on nuclear receptor NHR-49. Proc Natl Acad Sci U S A *102*, 13496-13501.

Viney, M.E., and Lok, J.B. (2007). *Strongyloides spp*. WormBook, 1-15.

Wang, Z., Zhou, X.E., Motola, D.L., Gao, X., Suino-Powell, K., Conneely, A., Ogata, C., Sharma, K.K., Auchus, R.J., Lok, J.B., *et al.* (2009). Identification of the nuclear receptor DAF-12 as a therapeutic target in parasitic nematodes. Proc Natl Acad Sci U S A *106*, 9138-9143.